

## Supporting Information

### Stronger Host-guest Binding Does Not Necessarily Give Brighter Particles: A Case Study on a Polymeric AIEE-tunable and Size-tunable Suprasphere

Linxian Xu,<sup>†</sup> Rongrong Wang,<sup>†</sup> Wei Cui,<sup>†</sup> Lingyun Wang,<sup>†</sup> Herbert Meier,<sup>\*,‡</sup> Hao Tang,<sup>\*,†</sup> and Derong Cao<sup>\*,†</sup>

<sup>†</sup>State Key Laboratory of Luminescent Materials and Devices, School of Chemistry and Chemical Engineering, South China University of Technology, Guangzhou 510641, China

<sup>‡</sup>Institute of Organic Chemistry, University of Mainz, D-55099 Mainz, Germany

#### Table of Contents

<a href="#">Experimental Procedures</a> .....	2
<a href="#">Supplementary Figures</a> .....	6
<a href="#">Supplementary Equations</a> .....	25
<a href="#">References</a> .....	30

## Experimental Procedures

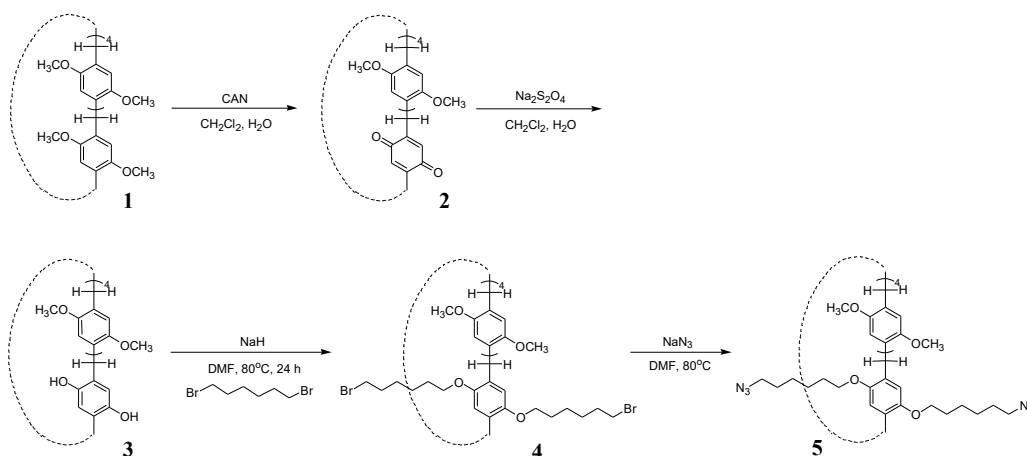
**General.** All solvents were obtained from commercial resources or dried according to the standard procedure. Other materials were purchased from Aladdin, Adamas and J&K and were used for synthesis without further purification.  $^1\text{H}$  NMR and  $^{13}\text{C}$  NMR spectra were collected on a Bruker DRX-400 spectrometer with tetramethylsilane used as reference. High resolution mass spectrometry (HRMS) was performed with a Bruker maXis impact instrument. Gel-permeation chromatography (GPC) analysis in THF was measured with a Waters ACQUITY advanced polymer chromatography system. Scanning electron microscope (SEM) was carried out on a Zeiss LEO1530VP field-emission scanning electron microscope system. Transmission electron microscopy (TEM) was operated on a JEOL JEM-2100F field emission transmission electron microscopy. Fluorescence spectra were recorded on a Hitachi F-4500 fluorescence spectrophotometer. Dynamic light scattering experiments were performed with a Malvern Zetasizer Nano ZS system. The dependence of particle concentration on the particle size for each **PASS** system was determined by the multispectral nanoparticle tracking analysis (m-NTA) technique enabled by the ViewSizer<sup>TM</sup> 3000 (MANTA Instruments, USA)<sup>1</sup> and was then used to calculate the relative particle density with the equations described below (see the section of Supplementary Equations).

**Electron microscopic sample preparation.** The supraspheres were prepared by adding the guests into **P1** acetone solution with specific concentrations; the samples were then prepared on the carbon support films (TEM) or glass sheets (SEM) by drop method and dried under the infrared lamp.

**Numerical analysis.** The binding constants ( $K$ ) and the relative fluorescence quantum yields ( $\Phi$ ) were calculated by non-linear fitting of the fluorescent titration experiments with software *Scientist 3* (Micromath, USA). The corresponding models used in the numerical analysis are listed in Supplementary Equations.

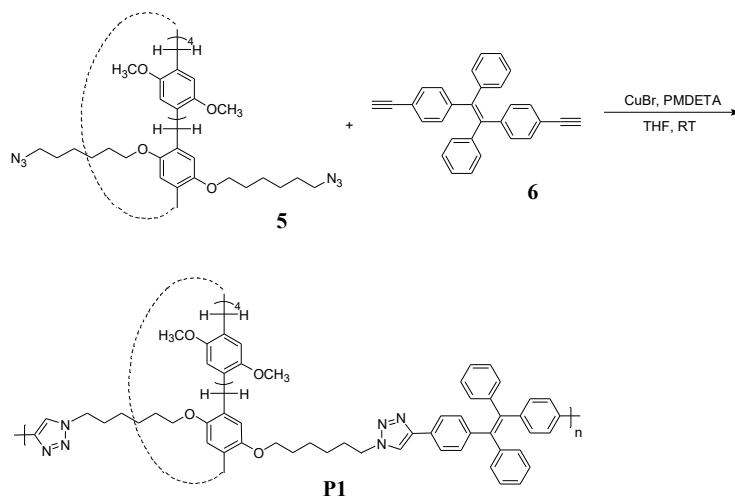
## Materials

1,4-Dimethoxypillar[5]arene and 1,2-bis(4-ethynylphenyl)-1,2-diphenylethene (**6**) were prepared according to the reported procedures<sup>2</sup>.

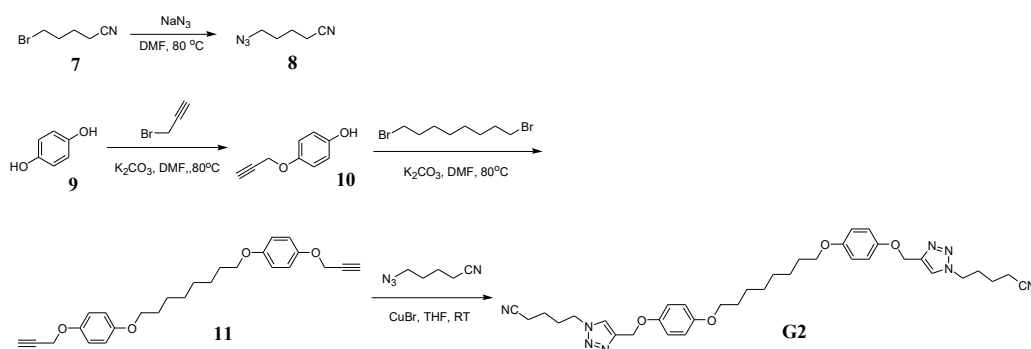


**Synthesis of monomer 5.** Dihydroxyl pillar[5]arene **3** (1445.6 mg, 2 mmol), 1,6-dibromohexane (1.5 mL, 10 mmol) and NaH (110.0 mg, 4.4 mmol) were dispersed in 30 mL DMF. The mixture was degassed with nitrogen and stirred under 80 °C overnight. The mixture was poured into water and extracted with dichloromethane. The crude product was concentrated under reduced pressure, then purified by column chromatography to get **4** as white powder (1783.2 mg, 1.7 mmol) in ~85% yield. Then, compound **4** (1048.9 mg, 1 mmol) was treated with  $\text{NaN}_3$  (195.0 mg, 3 mmol) in DMF under 80 °C for 12 h. The mixture was extracted by water and dichloromethane for 3 times. The organic phase was concentrated under vacuum and subjected to silica gel chromatography (petroleum ether / dichloromethane / ethyl acetate: 10 / 5 / 1) to give **5** as a white powder (895.2 mg, 92% yield). M.p. 179.5–180.0 °C.  $^1\text{H}$  NMR (400 MHz, acetone- $d_6$ , 298 K),  $\delta$  (ppm): 6.90 (s, 2H), 6.89 (s, 2H), 6.88 (s, 2H), 6.87 (s, 2H), 6.85 (s, 2H), 3.90 (t,  $J = 6.6$ , 4H), 3.76 (s, 6H), 3.76 (s, 6H), 3.75 (s, 6H), 3.74 (s, 6H), 3.72 (s, 10H), 3.05 (s, 4H), 1.86–1.79 (m,

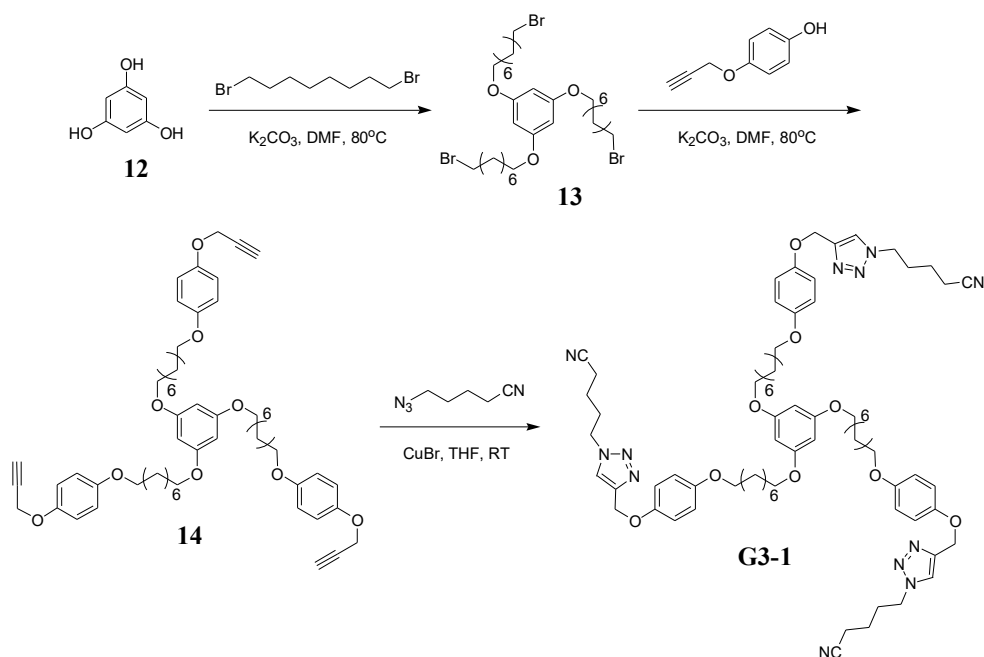
4H), 1.49–1.41 (m, 4H), 1.33–1.23 (m, 8H).  $^{13}\text{C}$  NMR (100 MHz,  $\text{CDCl}_3$ , 298 K),  $\delta$  (ppm): 150.8, 150.7, 150.5, 150.4, 149.8, 128.8, 128.3, 128.0, 114.5, 114.0, 113.9, 113.4, 113.2, 68.5, 56.1, 55.9, 55.7, 55.4, 55.3, 50.7, 30.1, 29.6, 29.5, 29.2, 27.5, 26.0, 25.1. HRMS:  $m/z$  calcd. for  $[\text{M}+\text{Na}]^+$   $\text{C}_{53}\text{H}_{68}\text{N}_6\text{NaO}_{10}$ : 995.4895; found 995.4889.



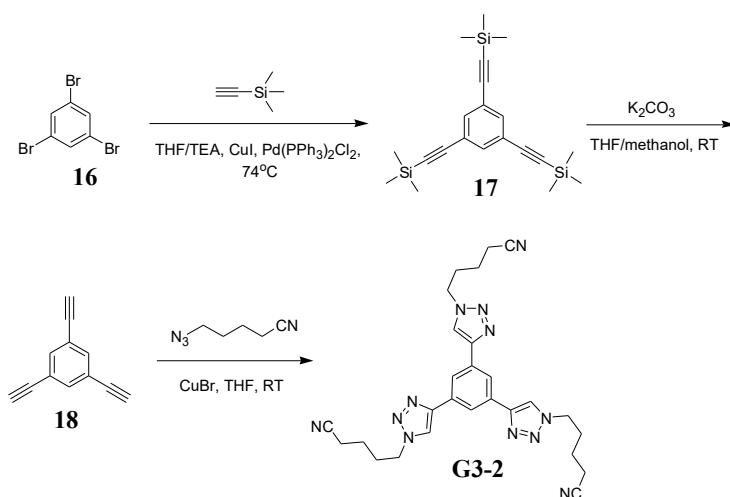
**Synthesis of host polymer P1.** Compound **5** (486.6 mg, 0.5 mmol), 1,2-bis(4-ethynylphenyl)-1,2-diphenylethene (**6**, 190.2 mg, 0.5 mmol), CuBr (7.2 mg, 0.05 mmol) and 1,1,4,7,7-pentamethyldiethylenetriamine (PMDETA, 17.3 mg, 0.1 mmol) were dissolved in 20 mL dry THF. The mixture was degassed and stirred under room temperature for 48 hours. The mixture was concentrated under reduced pressure, and then precipitated in methanol. The precipitate was purified by flash silicone gel column chromatography with THF as eluent. The target polymer **P1** was obtained by precipitation in methanol for 3 times and dried in vacuum under 55 °C as yellow-green powder (483.3 mg) in 71.4% yield.  $^1\text{H}$  NMR (400 MHz,  $\text{CDCl}_3$ , 298 K),  $\delta$  (ppm): 7.72–7.63 (m, 1H), 7.61–7.56 (m, 2H), 7.52–7.29 (m, 4H), 7.23–6.95 (m, 12H), 6.93–6.59 (m, 10H), 4.13–3.18 (m, 42H), 1.54–1.48 (m, 2H), 1.47–1.21 (m, 4H), 1.24–0.93 (m, 6H), 0.85–0.54 (m, 4H). As evaluated by gel-permeation chromatography (GPC), number-average molecular weight ( $M_n$ ) of **P1** is about  $1.0 \times 10^4$  g/mol, with the polydispersity index (PDI) of 2.19.



**Synthesis of guest G2.** Compound **11** (609.8 mg, 1.5 mmol) and 5-azido-pentanenitrile (**8**, 744.6 mg, 6 mmol) were added to 20 mL dry THF. CuBr (21.5 mg, 0.15 mmol) was introduced into the mixture and the mixture was degassed with  $\text{N}_2$ , then stirred at room temperature for 12 h. The crude product was concentrated under reduced pressure, then extracted with brine and  $\text{CH}_2\text{Cl}_2$  to get rid of CuBr. The organic phase was concentrated under reduced pressure and recrystallized in ethanol to produce the product **G2** as white needle-like crystal (884.0 mg, 1.35 mmol, 90% yield).<sup>3</sup> M.p. 120.2–121.8 °C.  $^1\text{H}$  NMR (400 MHz,  $\text{CDCl}_3$ , 298 K),  $\delta$  (ppm): 7.60 (s, 2H), 6.93–6.88 (m, 4H), 6.84–6.80 (m, 4H), 5.16 (s, 4H), 4.42 (t,  $J = 6.8$  Hz, 4H), 3.90 (t,  $J = 6.6$  Hz, 4H), 2.40 (t,  $J = 7.0$  Hz, 4H), 2.13–2.06 (m, 4H), 1.79–1.65 (m, 8H), 1.48–1.37 (m, 8H).  $^{13}\text{C}$  NMR (100 MHz,  $\text{CDCl}_3$ , 298 K),  $\delta$  (ppm): 153.8, 152.2, 144.8, 122.6, 118.9, 115.9, 115.4, 68.6, 62.7, 49.2, 29.3, 29.3, 29.0, 26.0, 22.3, 16.7. HRMS:  $m/z$  calcd. for  $[\text{M}+\text{Na}]^+$   $\text{C}_{36}\text{H}_{46}\text{N}_8\text{NaO}_4$ : 677.3540; found 677.3534.

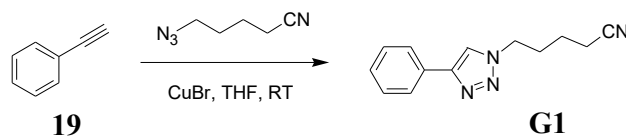


**Synthesis of guest G3-1.** Compound **14** (1153.2 mg, 1.3 mmol), 5-azido-pentanenitrile (**8**, 968.0 mg, 7.8 mmol) and  $CuBr$  (57.0 mg, 0.4 mmol) were added into 20 mL of degassed THF and protected in nitrogen atmosphere. The mixture was stirred under room temperature for 12 h, then poured into brine (100 mL) and extracted by dichloromethane. The organic layer was concentrated under vacuum, and recrystallized in ethanol to afford product **G3-1** (1424.6 mg, 1.13 mmol, 87% yield) as white powder.<sup>[2]</sup> M.p. 101.4–102.1 °C.  $^1H$  NMR (400 MHz,  $CDCl_3$ , 298 K),  $\delta$  (ppm): 7.59 (s, 3H), 6.92–6.88 (m, 6H), 6.84–6.80 (m, 6H), 6.06 (s, 3H), 5.15 (s, 6H), 4.41 (t,  $J = 6.6$  Hz, 6H), 3.92–3.88 (m, 12H), 2.39 (t,  $J = 6.8$  Hz, 6H), 2.12–2.05 (m, 6H), 1.79–1.64 (m, 18H), 1.47–1.35 (m, 24H).  $^{13}C$  NMR (100 MHz,  $CDCl_3$ , 298 K),  $\delta$  (ppm): 161.0, 153.8, 152.2, 144.9, 122.5, 118.9, 115.9, 115.5, 93.9, 68.58, 68.0, 62.8, 49.2, 29.4, 29.3, 29.3, 29.2, 29.0, 26.0, 26.0, 22.3, 16.7. HRMS:  $m/z$  calcd. for  $[M+Na]^+$   $C_{72}H_{96}N_{12}NaO_9$ : 1295.7321; found 1295.7315.

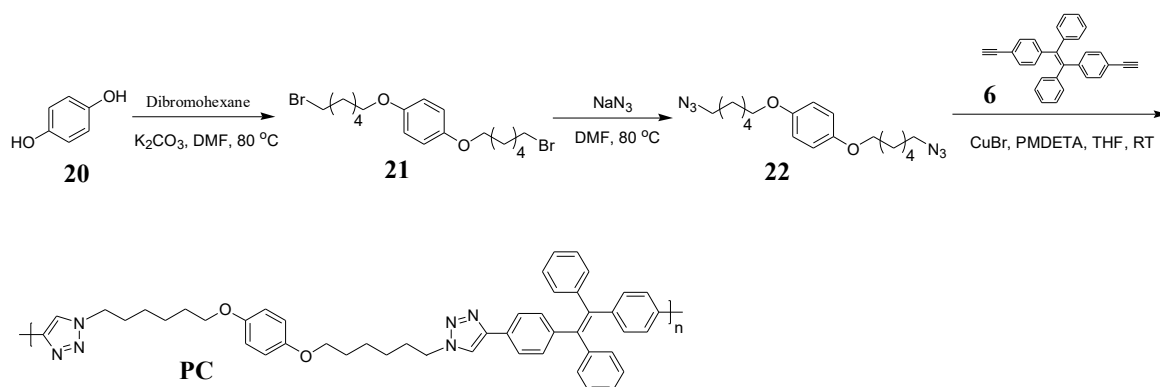


**Synthesis of guest G3-2.** 1,3,5-Triethynylbenzene (**18**, 211.0 mg, 1.4 mmol) and 5-azido-pentanenitrile (632.9 mg, 5.1 mmol) were added into 30 mL dry THF, and then  $CuBr$  (57.4 mg, 0.4 mmol) was introduced into the reaction mixture. The mixture was stirred at room temperature for 12 h under the protection of nitrogen. The crude product was concentrated under reduced pressure. The residue was washed by water, and then

extracted by CH<sub>2</sub>Cl<sub>2</sub>. The CH<sub>2</sub>Cl<sub>2</sub> phase was concentrated under vacuum and then recrystallized in ethanol to get **G3-2** (607.6 mg, 1.16 mmol, 83% yield) as white powder. M.p. 177.4–178.4 °C. <sup>1</sup>H NMR (400 MHz, CDCl<sub>3</sub>, 298 K), δ (ppm): 8.29 (s, 3H), 7.98 (s, 3H), 4.51 (t, J = 6.8 Hz, 6H), 2.45 (t, J = 7.0 Hz, 6H), 2.21–2.13 (m, 6H), 1.79–1.61 (m, 6H). <sup>13</sup>C NMR (100 MHz, CDCl<sub>3</sub>, 298 K), δ (ppm): 147.4, 131.7, 122.5, 120.2, 118.9, 49.4, 29.1, 22.4, 16.7. HRMS: m/z calcd. for [M+Na]<sup>+</sup> C<sub>27</sub>H<sub>30</sub>N<sub>12</sub>Na: 545.2614; found 545.2609.



**Synthesis of guest G1.** Ethynyl-benzene (**19**, 204.3 mg, 2 mmol), 5-azido-pentanenitrile (298.0 mg, 2.4 mmol), and CuBr (28.7 mg, 0.2 mmol) were added into 20 mL degassed THF. The mixture was stirred under room temperature for 12 h, and then concentrated under vacuum. The crude product was obtained by extraction with CH<sub>2</sub>Cl<sub>2</sub> and concentration under vacuum. Then the crude product was further purified by recrystallization in ethanol to afford **G1** (209.0 mg, 0.92 mmol) as white fibrous. Yield: 46%. M.p. 59.6–60.2 °C. <sup>1</sup>H NMR (400 MHz, CDCl<sub>3</sub>, 298 K), δ (ppm): 7.83–7.80 (m, 2H), 7.79 (s, 1H), 7.43–7.40 (m, 2H), 7.35–7.31 (m, 1H), 4.42 (t, J = 7.0 Hz, 2H), 2.37 (t, J = 7.0 Hz, 2H), 2.12–2.04 (m, 2H), 1.71–1.63 (m, 2H). <sup>13</sup>C NMR (100 MHz, CDCl<sub>3</sub>, 298 K), δ (ppm): 147.9, 130.5, 128.9, 128.3, 125.7, 119.7, 119.0, 49.2, 29.1, 22.3, 16.7. HRMS: m/z calcd. for [M+Na]<sup>+</sup> C<sub>13</sub>H<sub>14</sub>N<sub>4</sub>Na: 249.1116; found 249.1111.



**Synthesis of control polymer PC.** 1,4-Bis-(6-bromo-hexyloxy)-benzene (**21**, 872.4 mg, 2 mmol) and 5-azido-pentanenitrile (260 mg, 4 mmol) were dispersed in 30 mL DMF, and then degassed with nitrogen and stirred under 80 °C for 12 h. Mixture was poured into water and then extracted with dichloromethane. The crude product was concentrated under reduced pressure, then purified by column chromatography (petroleum ether / ethyl acetate: 5 / 1) to afford compound **22** as white powder (648.8 mg, 1.8 mmol) with 90% yield. <sup>1</sup>H NMR (400 MHz, CDCl<sub>3</sub>, 298 K), δ (ppm): 6.81 (s, 4H), 3.91 (t, J = 6.4 Hz, 4H), 3.28 (t, J = 7.0 Hz, 4H), 1.80–1.73 (m, 4H), 1.65–1.60 (m, 4H), 1.56–1.42 (m, 8H). <sup>13</sup>C NMR (100 MHz, CDCl<sub>3</sub>, 298 K), δ (ppm): 153.2, 115.4, 68.4, 51.4, 29.3, 28.8, 26.5, 25.7.

Compound **22** (180.2 mg, 0.5 mmol), 1,2-bis(4-ethynylphenyl)-1,2-diphenylethene (**6**, 190.2 mg, 0.5 mmol), CuBr (7.2 mg, 0.05 mmol) and 1,1,4,7,7-pentamethyl-diethylenetriamine (PMDETA, 17.3 mg, 0.1 mmol) were dispersed in 20 mL dry THF, then degassed and stirred under room temperature for 48 hours. The mixture was concentrated under reduced pressure, and then precipitated in methanol. The precipitate was purified by flash silicone gel column chromatography with THF as eluent. The target polymer **PC** was obtained by precipitation in methanol as yellow-green powder (190.4 mg). Yield: 51.4 %. <sup>1</sup>H NMR (400 MHz, CDCl<sub>3</sub>, 298 K) δ (ppm): 7.64–7.64 (m, 2H), 7.59–7.53 (m, 3H), 7.17–6.95 (m, 15H), 6.81–6.75 (m, 4H), 4.36 (s, broad, 4H), 3.89–3.86 (m, 4H), 1.93 (s, broad, 4H), 1.73 (s, broad, 4H), 1.50 (s, broad, 4H), 1.39 (s, broad, 4H).

## Supplementary Figures

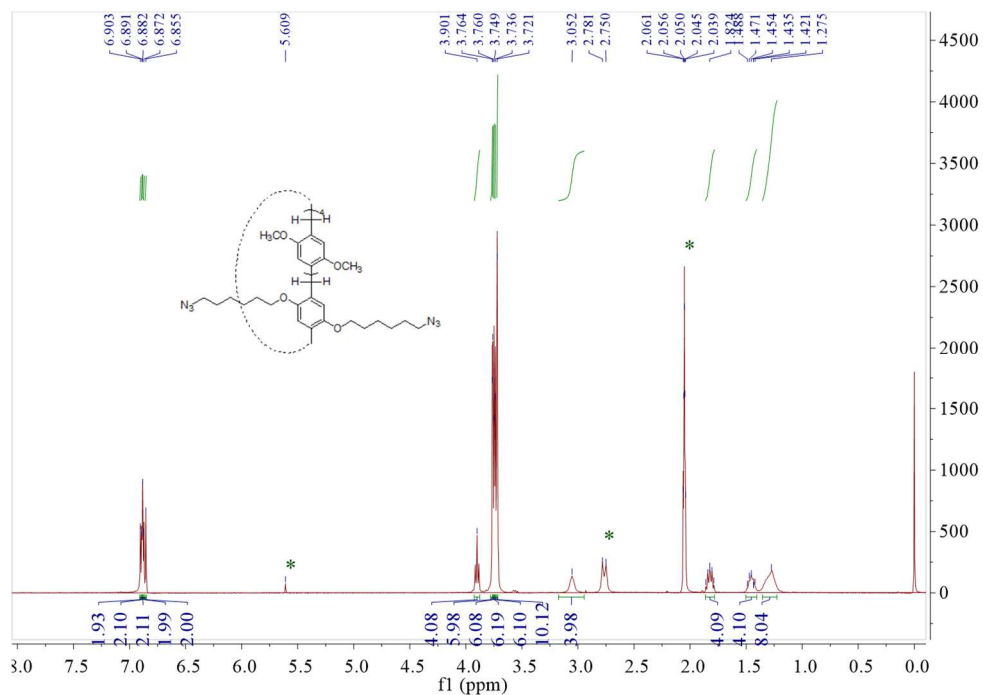


Figure S1. <sup>1</sup>H NMR spectrum of compound **5** (400 MHz, acetone-*d*<sub>6</sub>, 298 K).

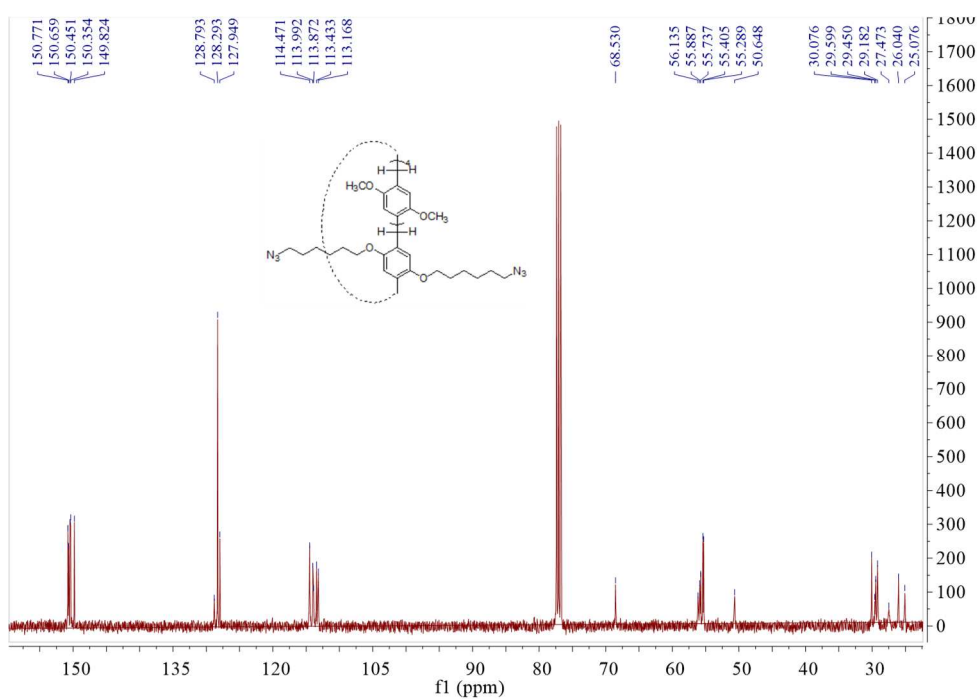


Figure S2. <sup>13</sup>C NMR spectrum of compound **5** (100 MHz, CDCl<sub>3</sub>, 298 K).

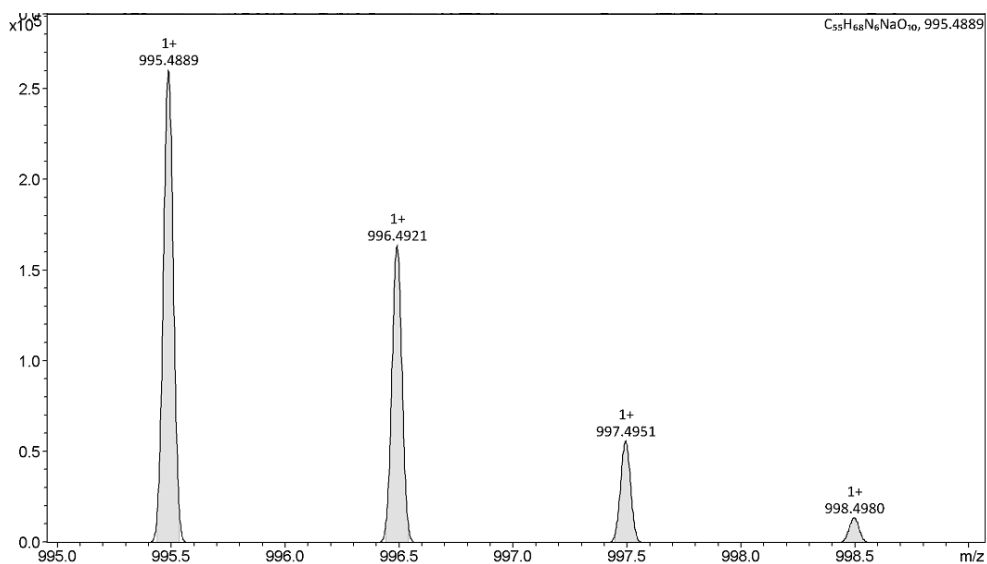


Figure S3. HRMS (ESI) spectrum of compound 5.

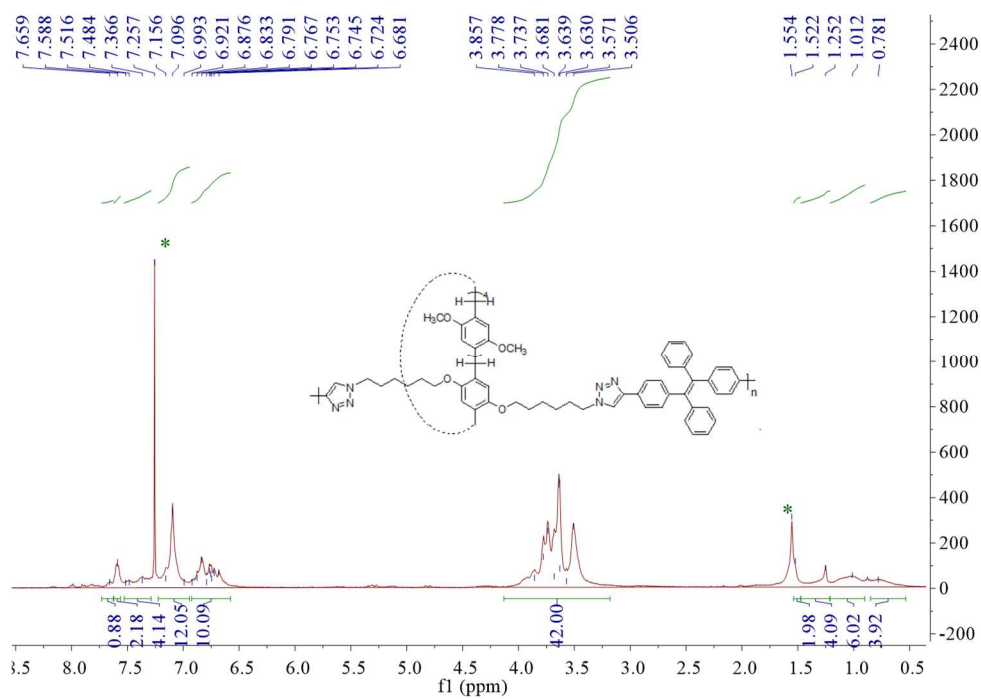


Figure S4.  $^1H$  NMR spectrum of P1 (400 MHz,  $CDCl_3$ , 298 K).

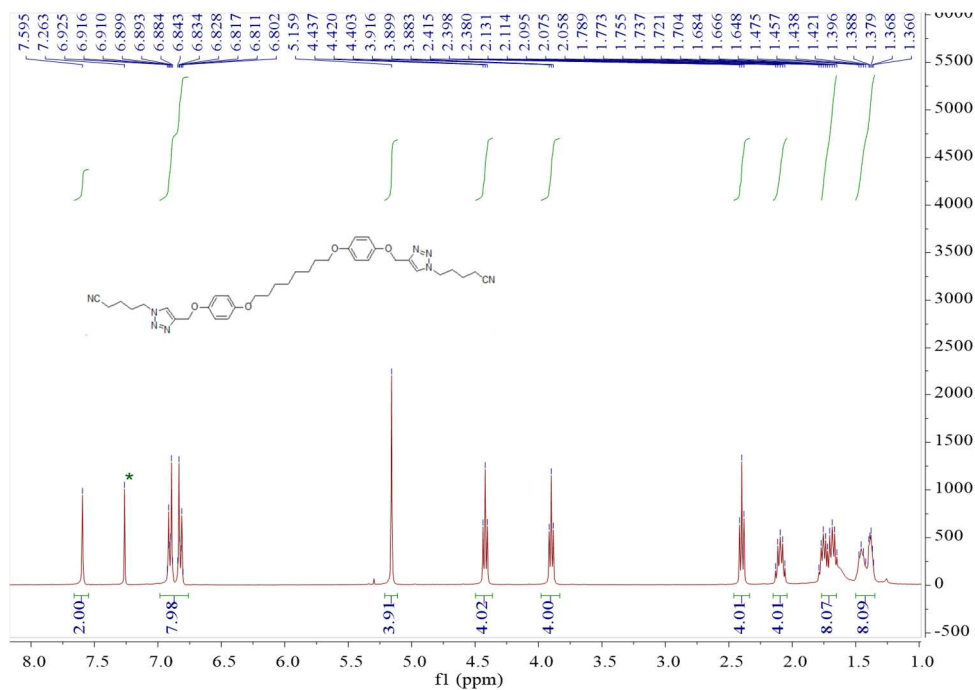


Figure S5.  $^1\text{H}$  NMR spectrum of guest G2 (400 MHz,  $\text{CDCl}_3$ , 298 K).

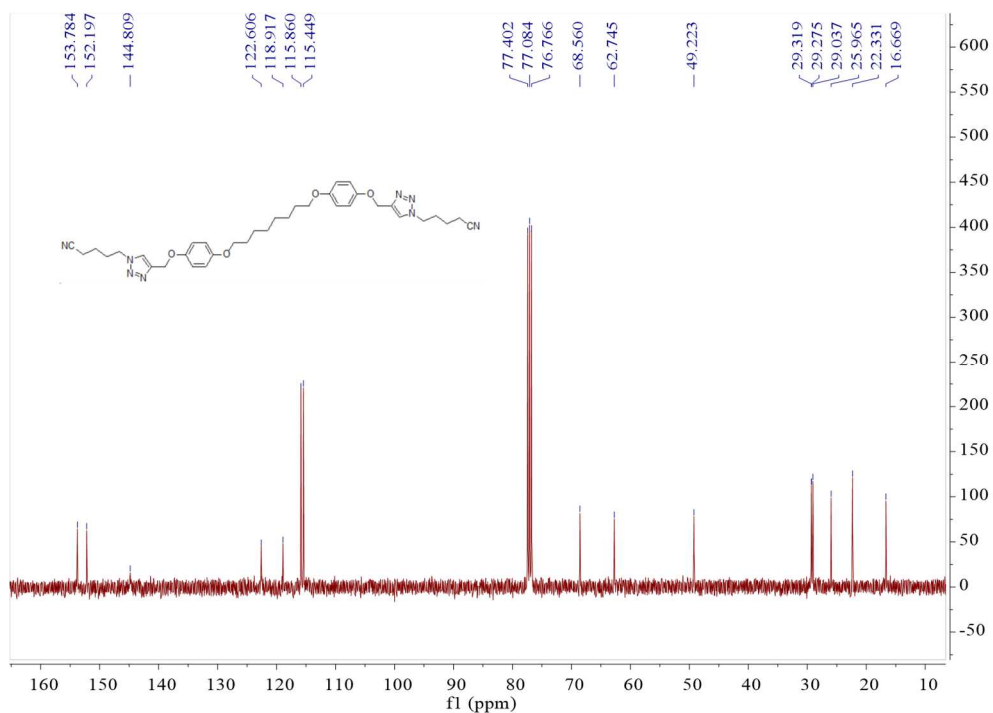


Figure S6.  $^{13}\text{C}$  NMR spectrum of guest G2 (100 MHz,  $\text{CDCl}_3$ , 298 K).



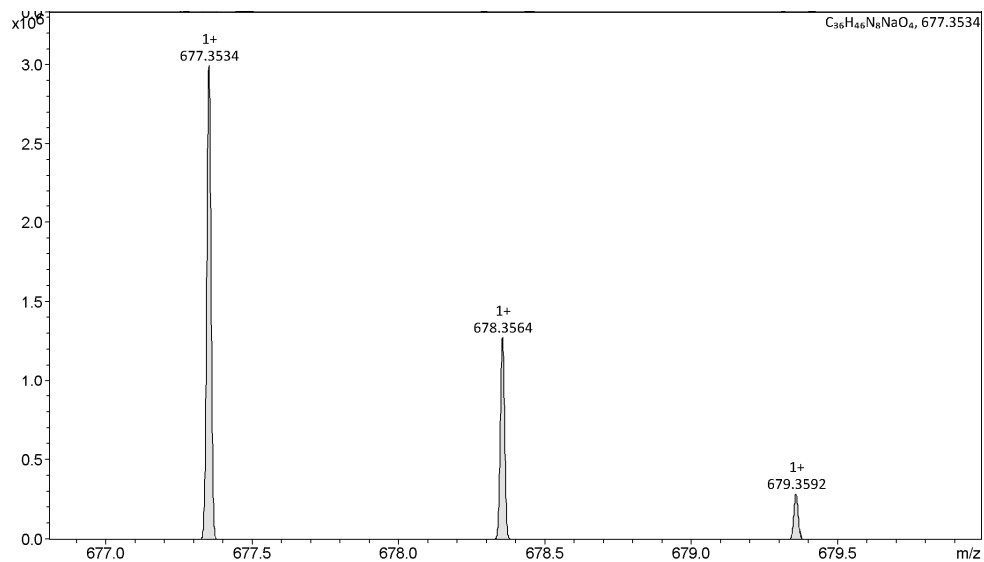


Figure S7. HRMS (ESI) spectrum of G2.

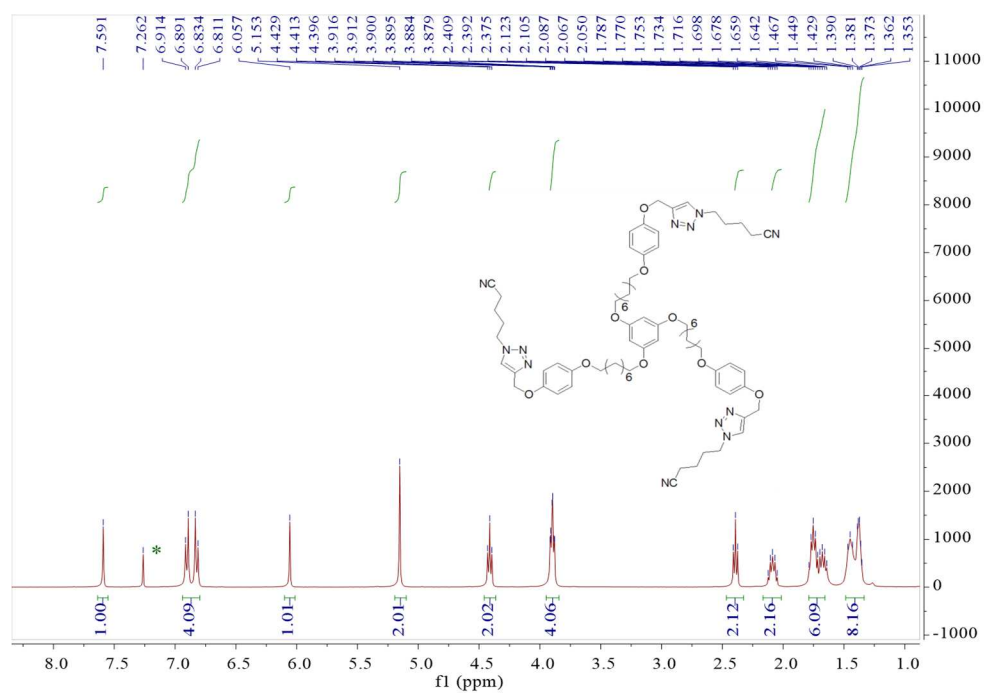


Figure S8. <sup>1</sup>H NMR spectrum of guest G3-1 (400 MHz, CDCl<sub>3</sub>, 298 K).

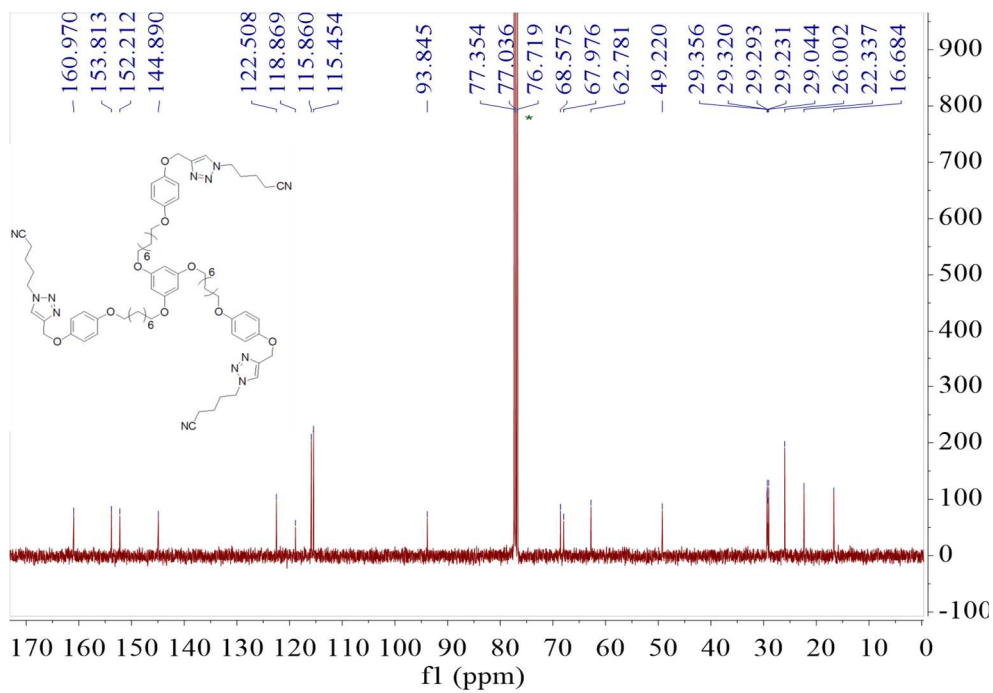


Figure S9.  $^{13}\text{C}$  NMR spectrum of guest **G3-1** (100 MHz,  $\text{CDCl}_3$ , 298 K).

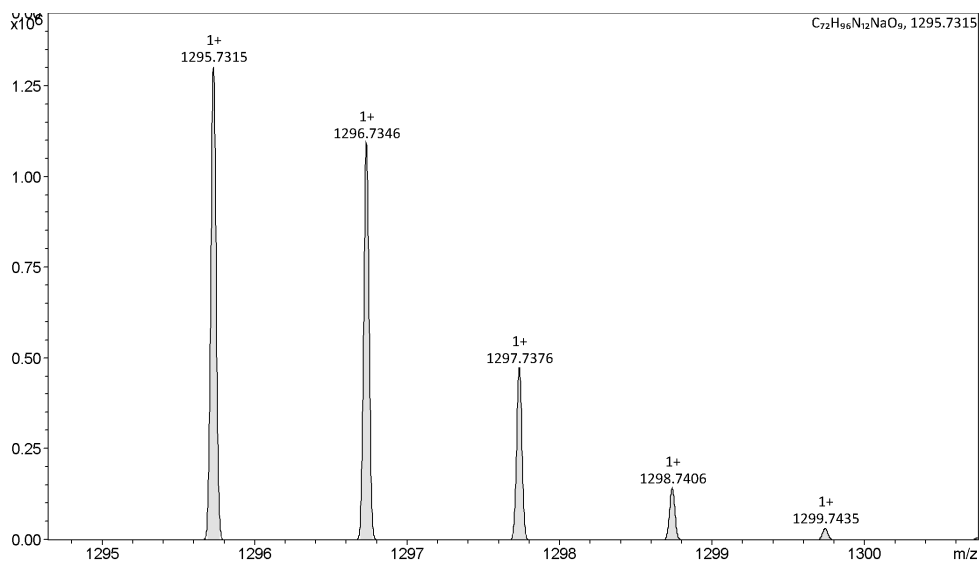


Figure S10. HRMS (ESI) spectrum of **G3-1**.

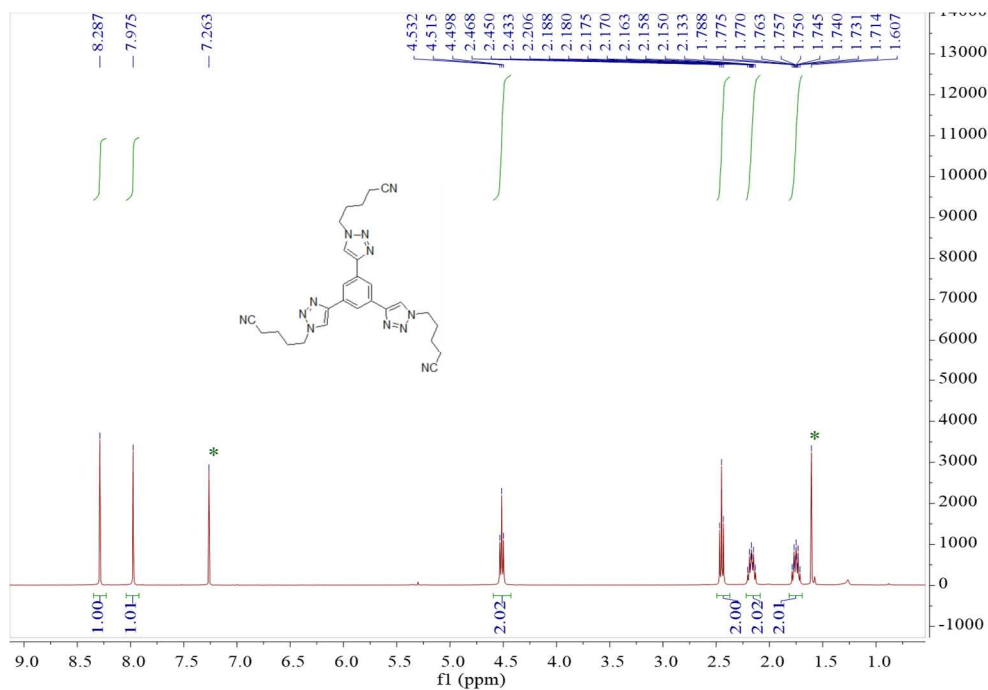


Figure S11.  $^1\text{H}$  NMR spectrum of guest G3-2 (400 MHz,  $\text{CDCl}_3$ , 298 K).

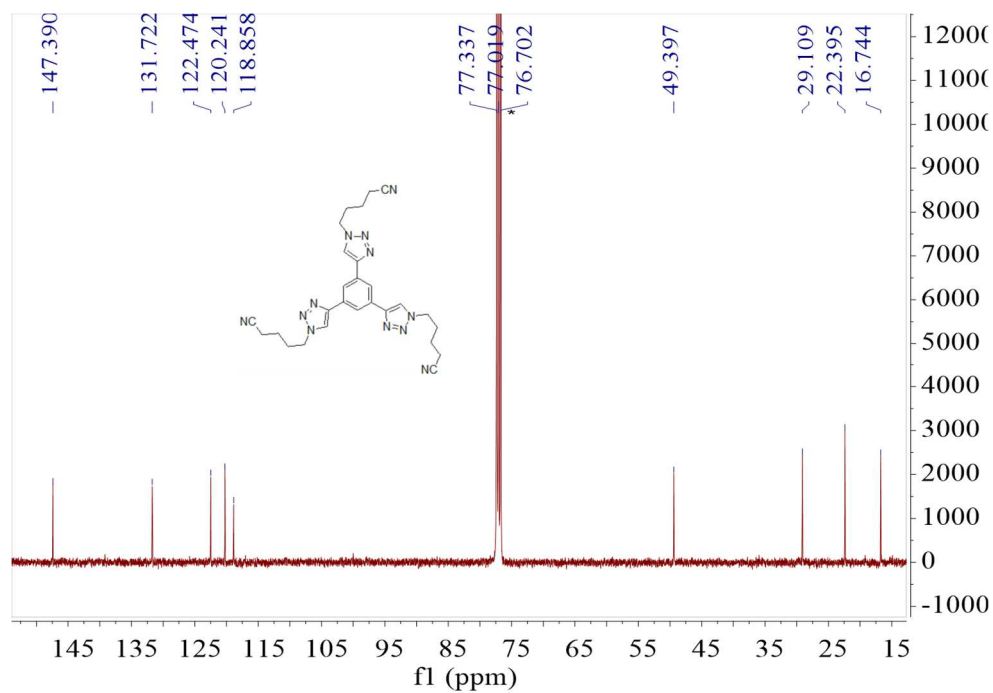


Figure S12.  $^{13}\text{C}$  NMR spectrum of guest G3-2 (100 MHz,  $\text{CDCl}_3$ , 298 K).

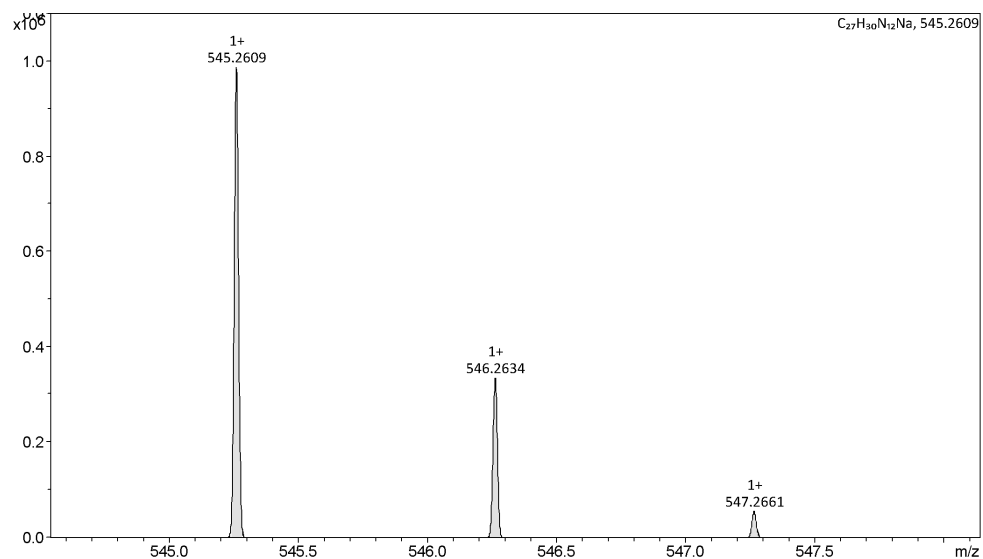


Figure S13. HRMS (ESI) spectrum of G3-2.

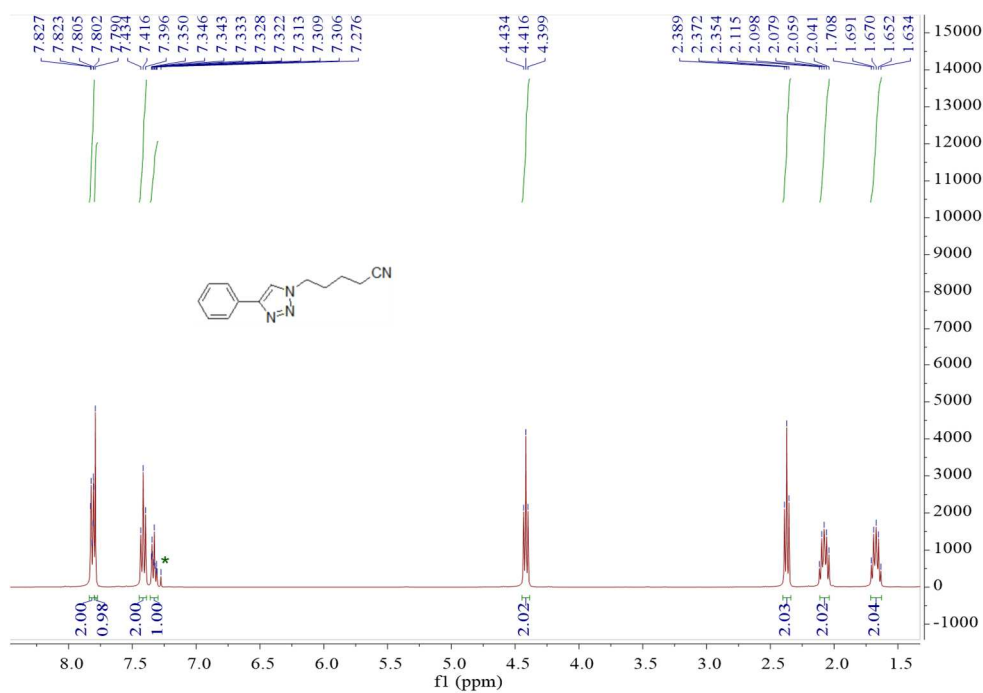


Figure S14.  $^1H$  NMR spectrum of guest G1 (400 MHz,  $CDCl_3$ , 298 K).

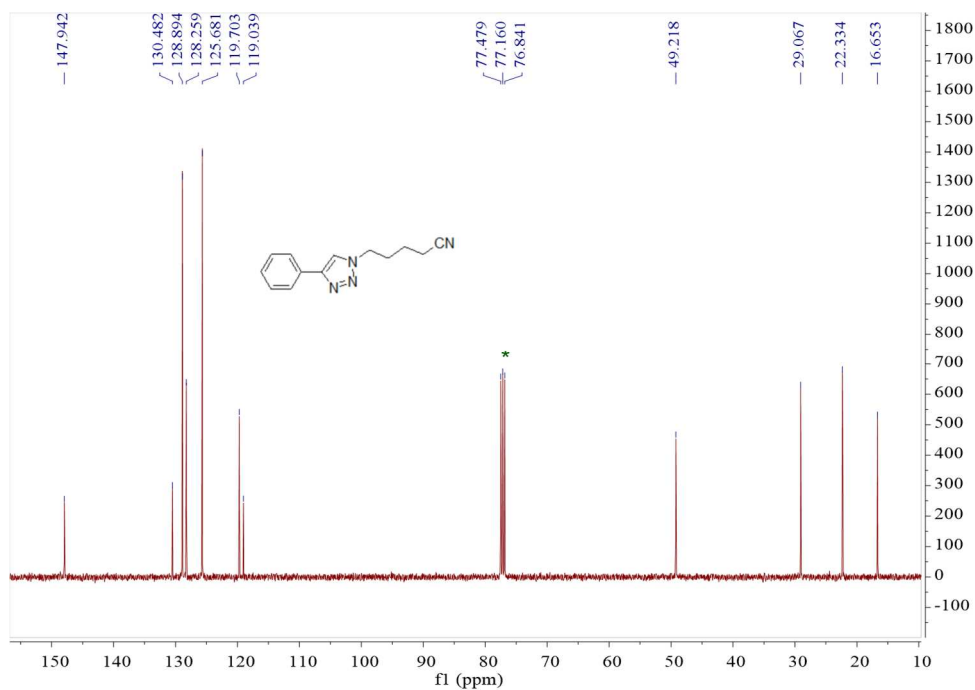


Figure S15.  $^{13}\text{C}$  NMR spectrum of guest G1 (100 MHz,  $\text{CDCl}_3$ , 298 K).

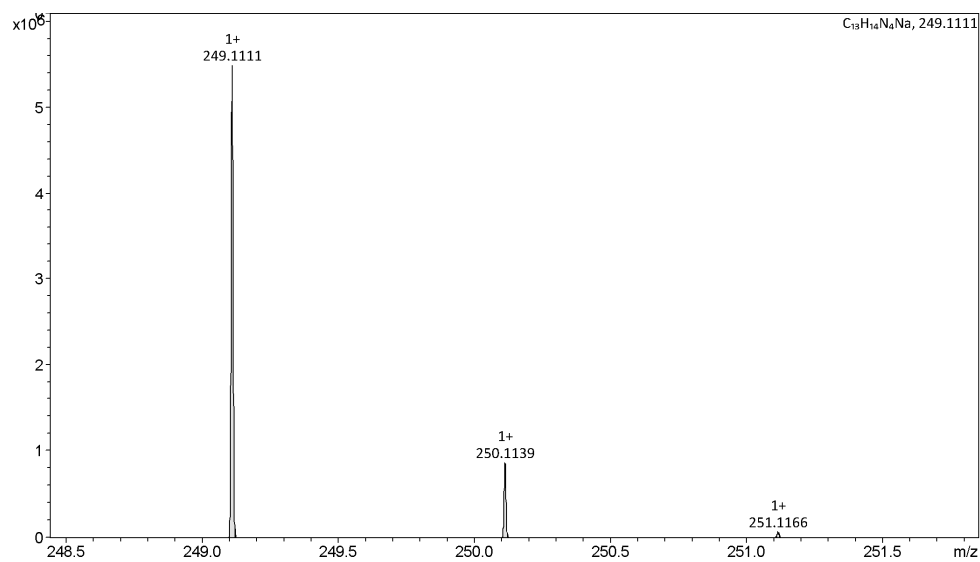
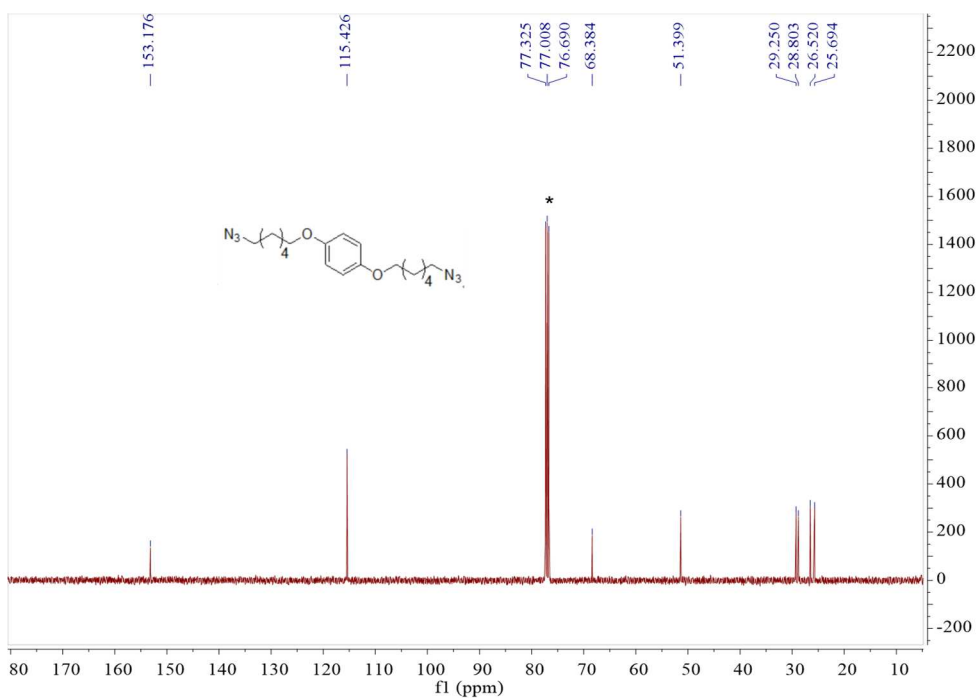
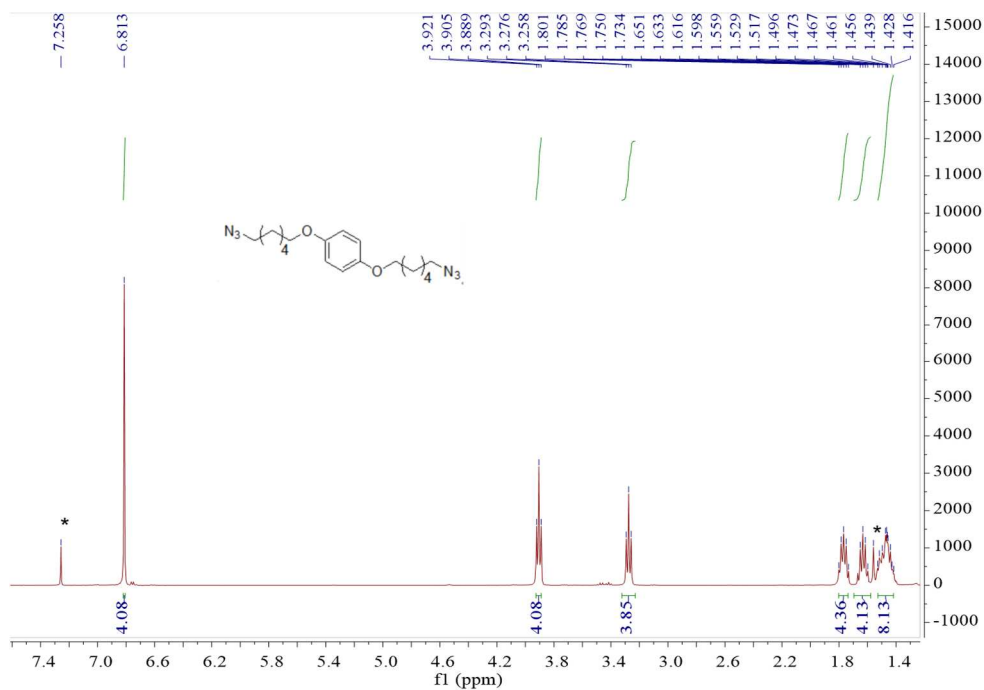
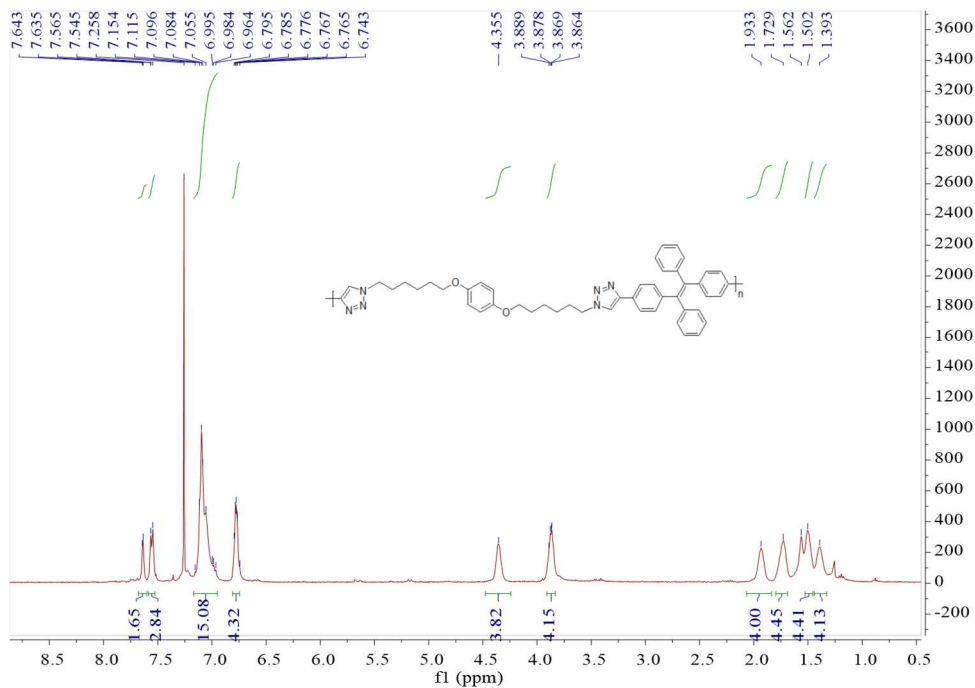
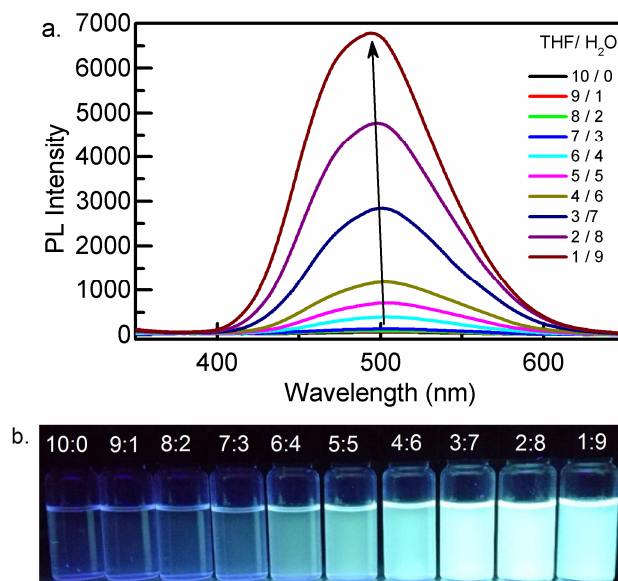


Figure S16. HRMS (ESI) spectrum of G1.





**Figure S19.**  $^1\text{H}$  NMR spectrum of polymer PC (400 MHz,  $\text{CDCl}_3$ , 298 K).



**Figure S20.** (a) Fluorescence spectra of P1 in THF–water mixtures with different solvent ratios ( $\lambda_{\text{ex}}=340$  nm); (b) The corresponding fluorescence under a UV lamp (365 nm).  $[\text{RU}] = 10 \mu\text{M}$ .

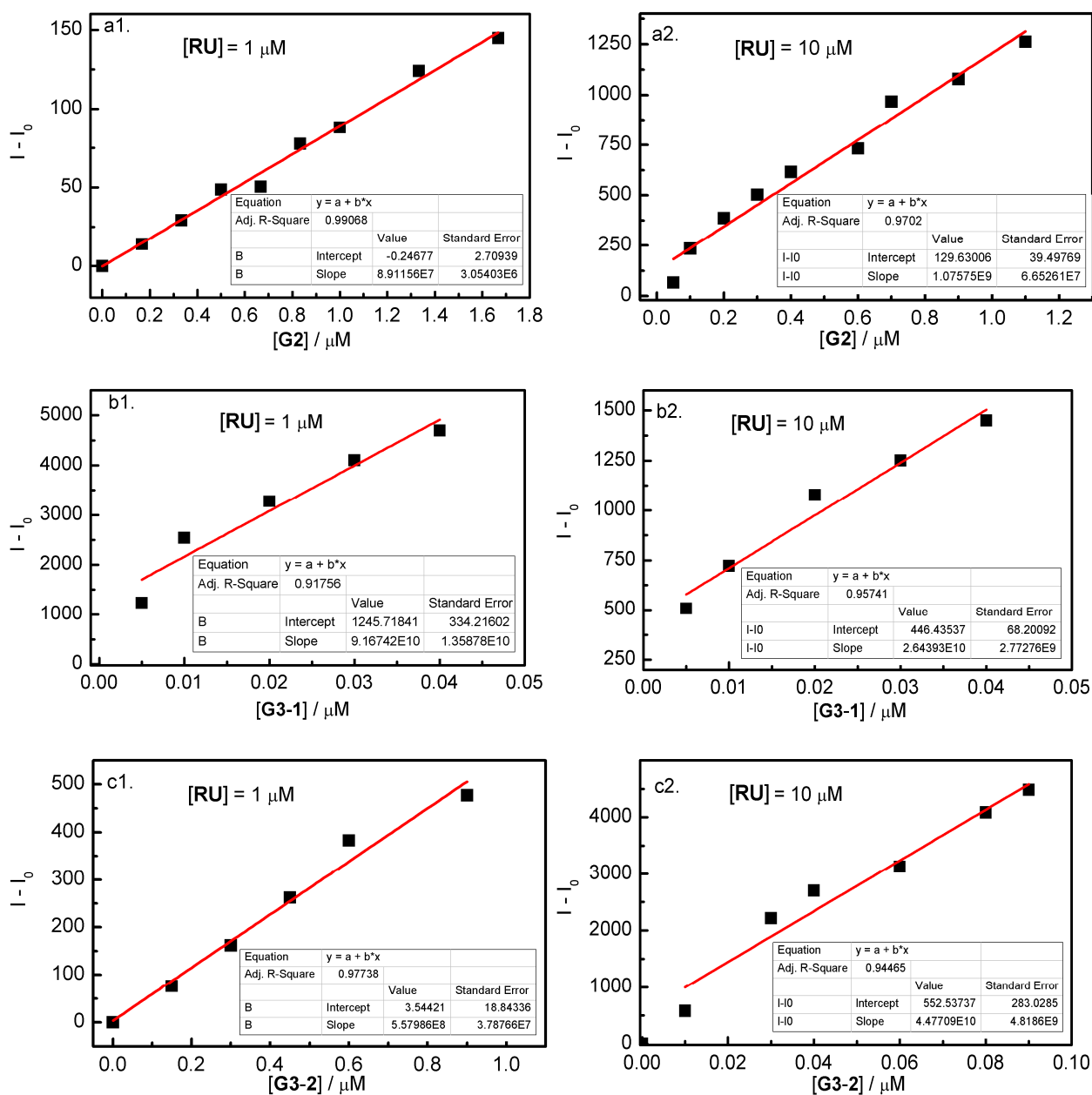


**Figure S21.** Limit of detection (LOD) for the binding of P1 towards GMs. GMs = G2 (a1, a2), G3-1 (b1, b2) and G3-2 (c1, c2).

LOD for the binding P1 towards G2, G3-1 or G3-2 was evaluated by the following equation ( $3\sigma$  criterion), where ' $\sigma$ ' was the standard deviation of the blank test (N=20).

$$\text{LOD} = 3\sigma / \text{Slope}$$



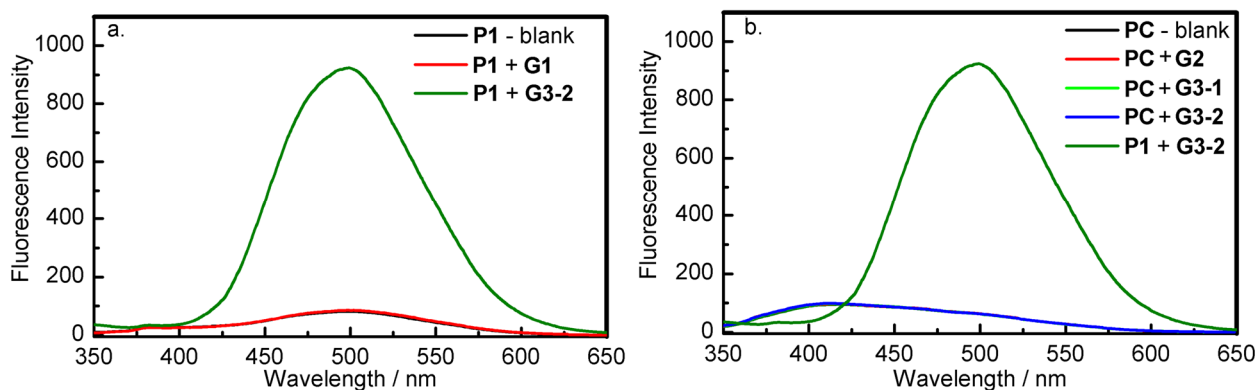


**Figure S22.** Fluorescence response of **P1** or **PC** toward the guests: (a) Fluorescence response of **P1** toward the monotopic guest **G1** in acetone; (b) Fluorescence response of **PC** toward the multitopic guests **G2**, **G3-1** and **G3-2** in acetone. The spectra of **P1** in the presence of **G3-2** were used for comparison.  $[\text{RU}] = 10 \mu\text{M}$ .  $[\text{GM}] = 16.7 \mu\text{M}$ .  $\lambda_{\text{ex}} = 340 \text{ nm}$ .

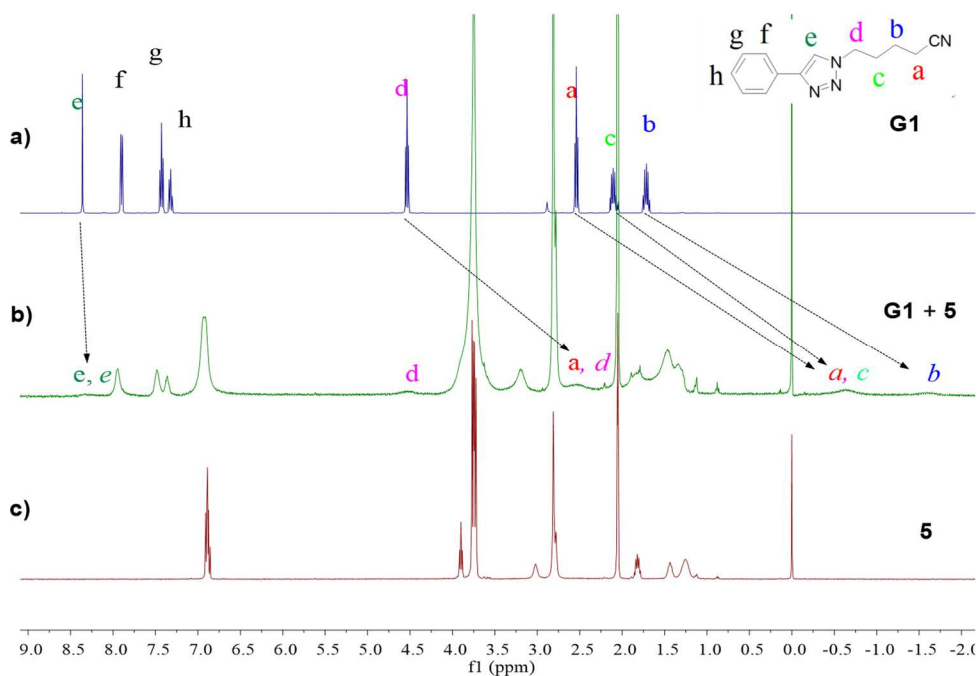


**Figure S23.**  $^1\text{H}$ NMR spectra for the binding of compound **5** with guest **G1**.  $^1\text{H}$  NMR spectra of **G1** (a), compound **5** (c) and the mixture of **G1** and compound **5** at 1:1 (b) were determined using  $\text{C}_3\text{D}_6\text{O}$  as solvent (400 MHz, 298 K).  $[\text{Compound } 5] = 0.05 \text{ M}$ .  $[\text{G1}] = 0.05 \text{ M}$ .

The alkyl protons *a*, *b*, *c*, *d* and triazole protons *e* of the guest **G1** shifted upfield upon the binding to the compound **5**. Meanwhile, the signal peaks of compound **5** were widened during the complexation process. Due to the slow chemical exchange between the guests free in solvent and bound as the complex, the signals for both guest species can be simultaneously observed.

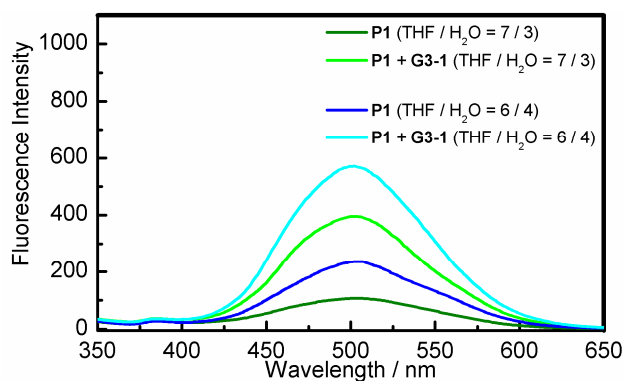


**Figure S24.** Fluorescence response of the aggregated **P1** towards guests in the mixture of THF and water.  $[RU] = 10 \mu\text{M}$ .  $[G] = 16.7 \mu\text{M}$ .  $\lambda_{\text{ex}} = 340 \text{ nm}$ .

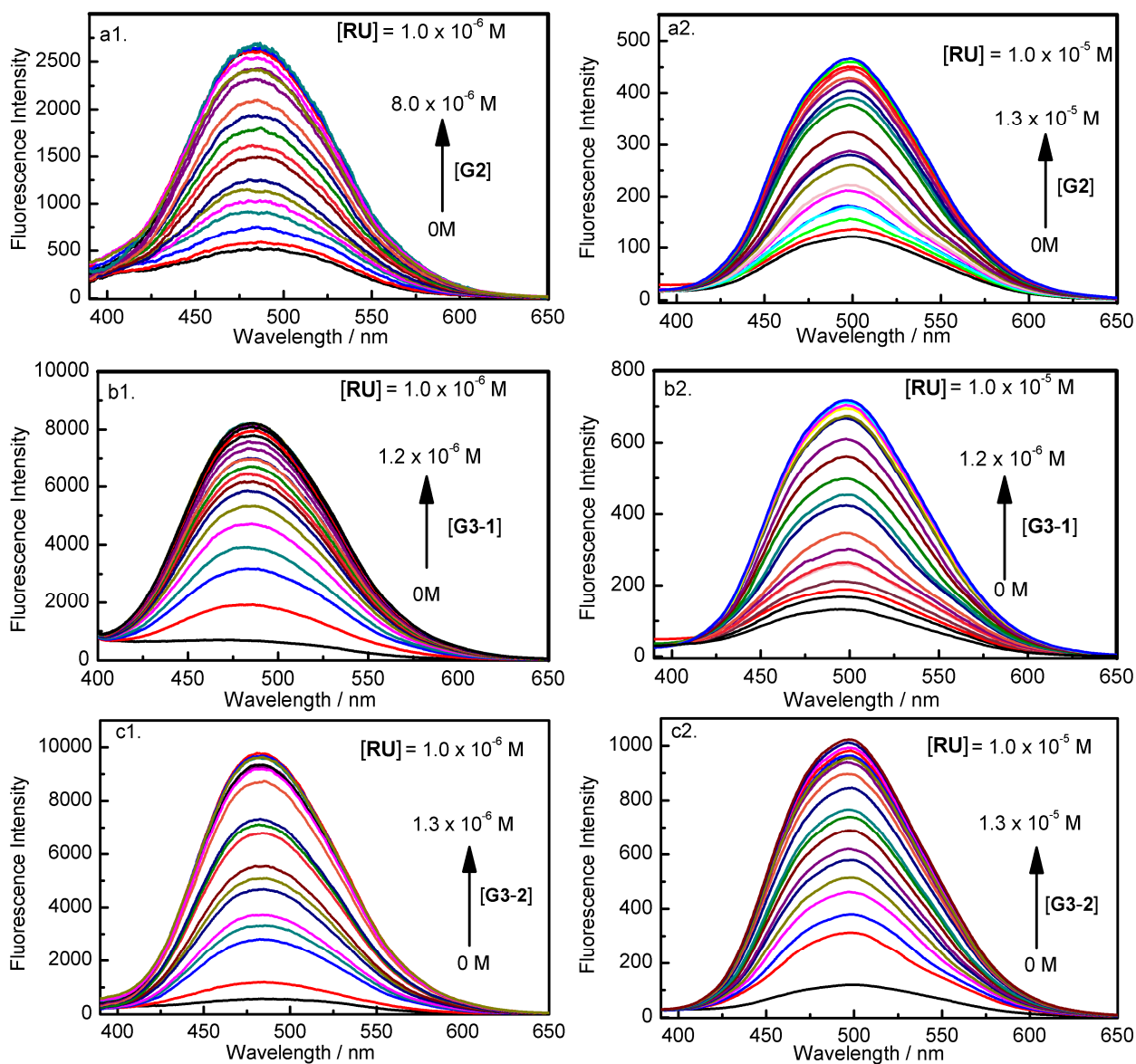


**Figure S25.** Dependence of Fluorescence of **P1** on the concentration of GMs in acetone. GMs = **G2** (a1, a2), **G3-1** (b1, b2) and **G3-2** (c1, c2),  $\lambda_{\text{ex}} = 340 \text{ nm}$ ,  $[RU] = 1 \mu\text{M}$  (a1, b1 and c1) or  $10 \mu\text{M}$  (a2, b2 and c2).

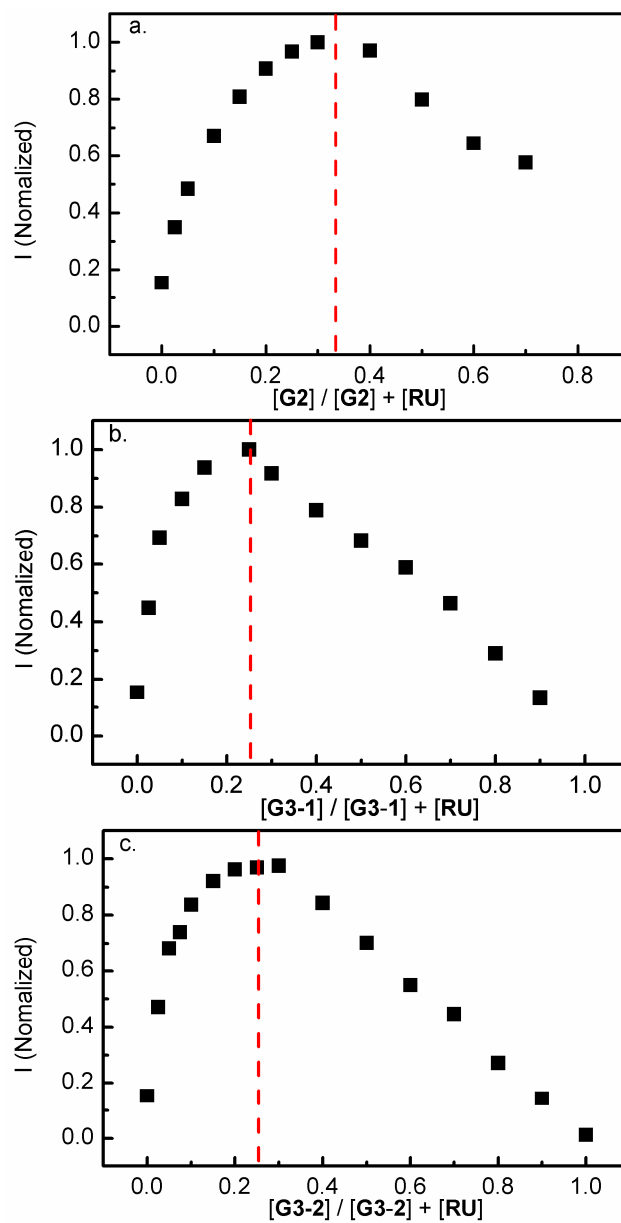
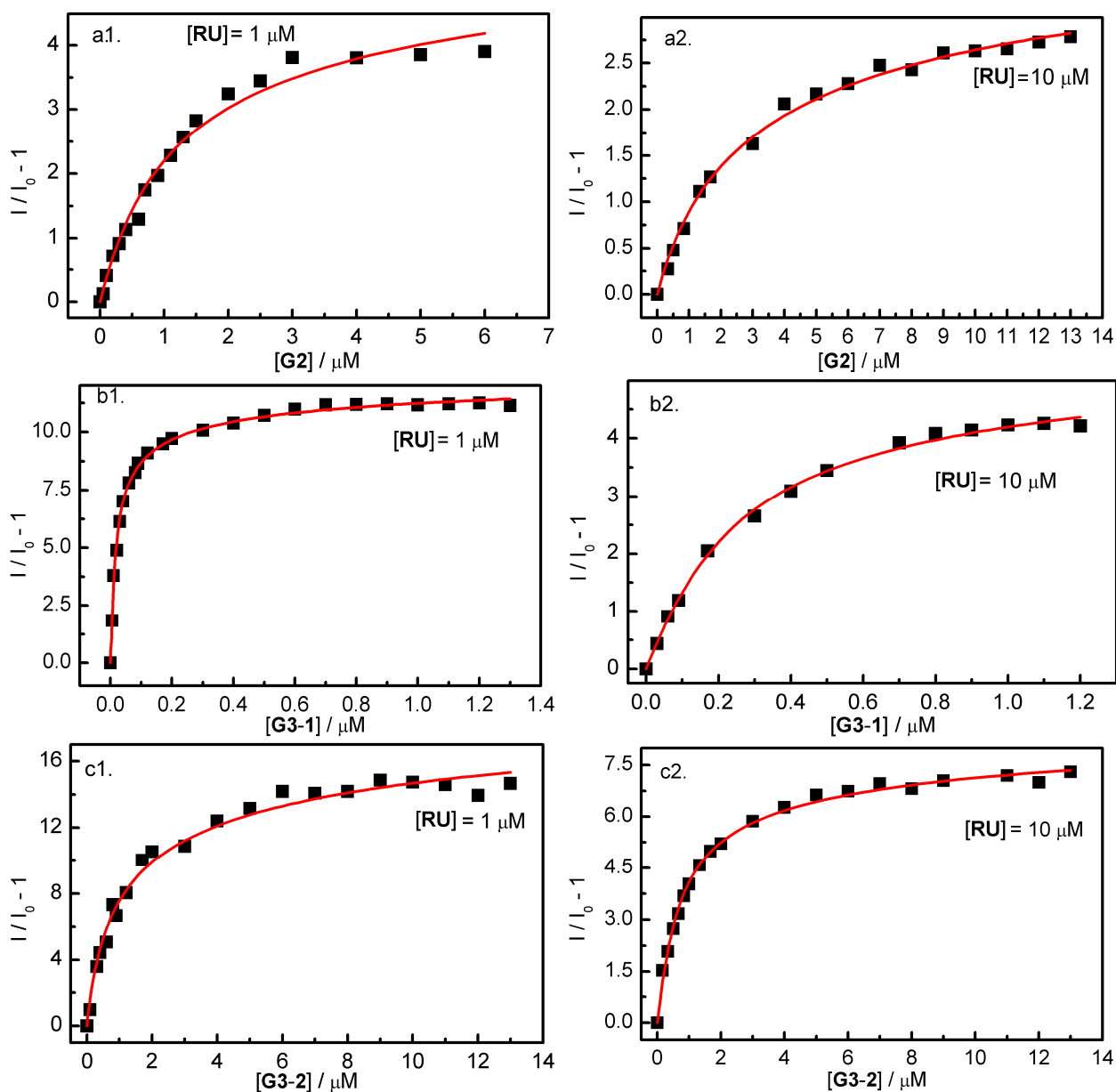
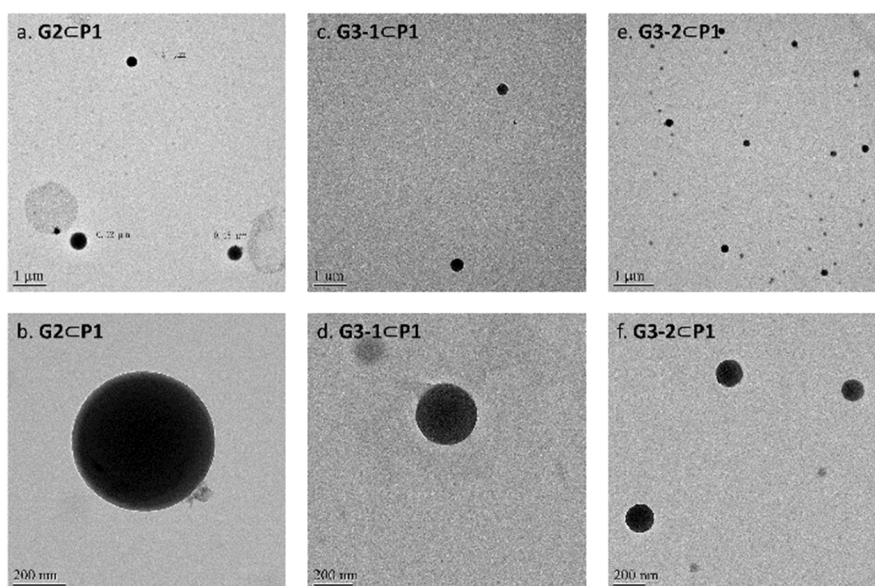


Figure S26. Job plots for the binding of RU to G2 (a), G3-1 (b) and G3-2 (c).



**Figure S27.** Non-linear fitting of the binding isotherm with different binding models. The data in panels **a1** and **a2** were for guest **G2** and fitted with a **RU:G2 2:1** model; figures **b1** and **b2** were for guest **G3-1** and fitted with a **RU:G3 3:1** model; figures **c1** and **c2** were for guest **G3-2** and fitted with a **RU:G3 3:1** model. The fluorescence intensities were integrated from 450 nm to 550 nm in the fluorescence spectra.



**Figure S28.** TEM images of the PASS for G2C-P1 (a, b), G3-1C-P1 (c,d) and G3-2C-P1 (e, f). [RU] = 10 μM. [GM] = 16.7 μM, .

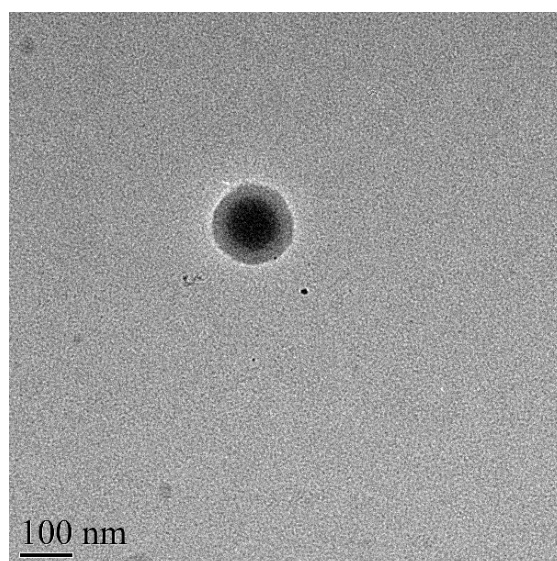


**Figure S29.** TEM images of the PASS at very low concentration of guest. [RU] = 10 μM. [G3-2] =  $1 \times 10^{-4}$  μM.

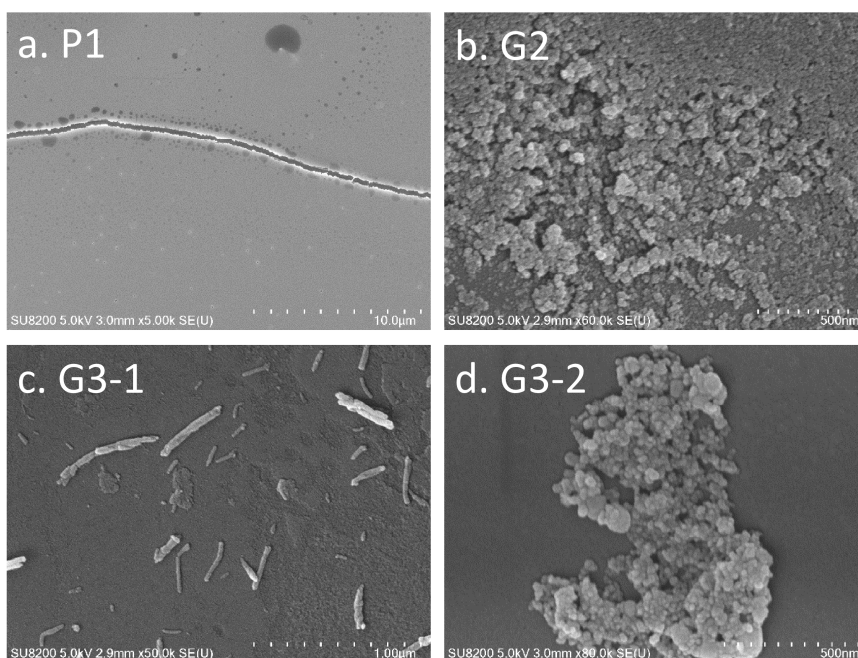


Figure S30. SEM images of P1 (a), G2 (b), G3-1 (c) and G3-2 (d).

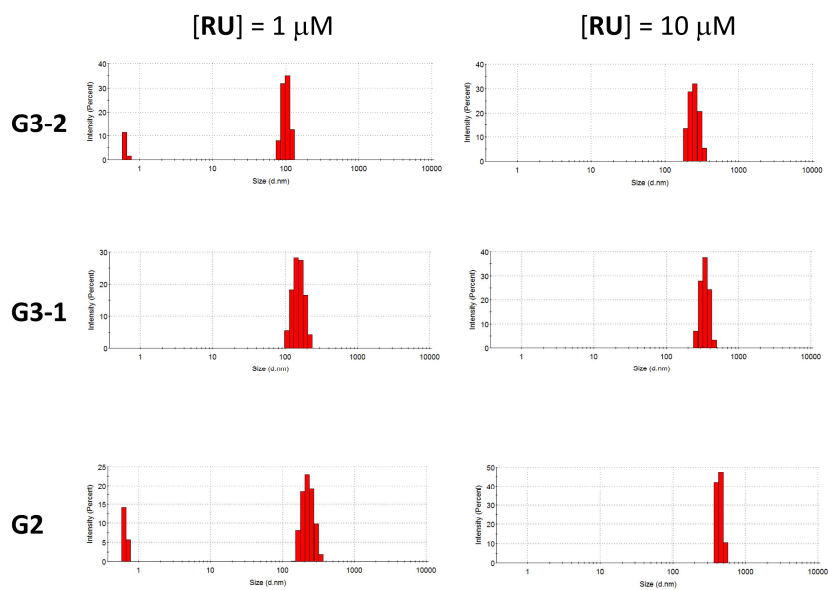
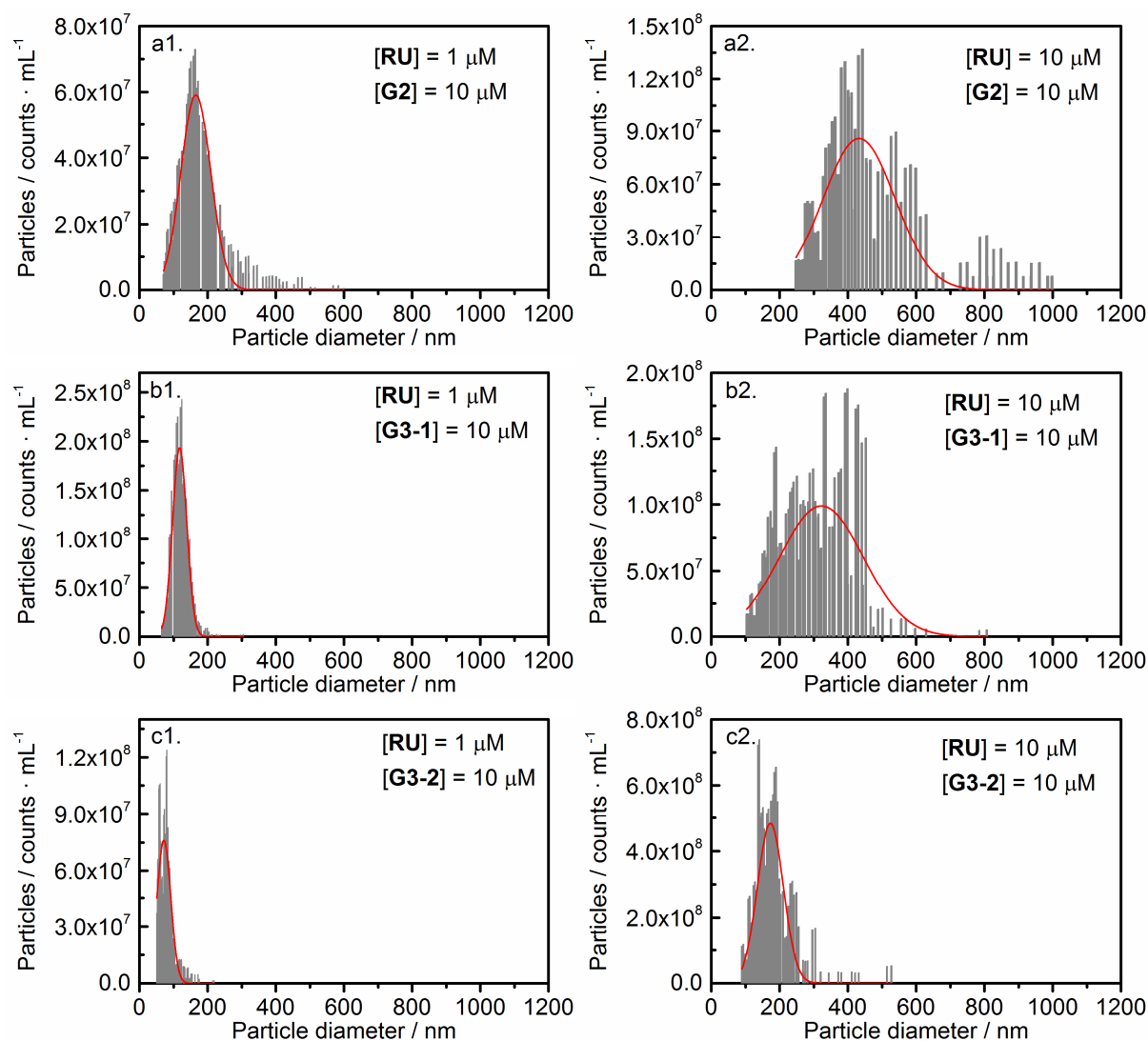
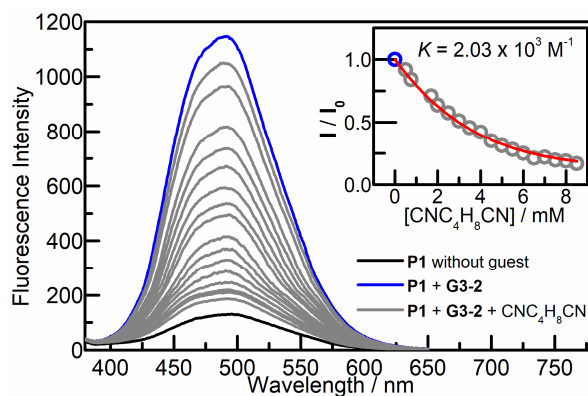


Figure S31. DLS experiments for PASS at different concentrations of P1 with different guests used. [GM] = 10 μM.



**Figure S32.** Results determined by the multispectral nanoparticle tracking analysis (m-NTA): Particle concentration and size distribution of **PASS** in acetone. **GM** = **G2** (a1, a2), **G3-1** (b1, b2) and **G3-2** (c1, c2). **[GMs]** = 10  $\mu\text{M}$ . **[RU]** = 1  $\mu\text{M}$  (a1, b1 and c1) or 10  $\mu\text{M}$  (a2, b2 and c2). The data were fitted with the Gauss distribution (red curves) to determine the average diameter of the nanoparticles.



**Fig. S33.** Fluorescent titration of **G3-2** with **P1** in acetone. Inset: fit of the binding isotherm. **[RU]** = 10  $\mu\text{M}$ , **[G3-2]** = 16.7  $\mu\text{M}$ .

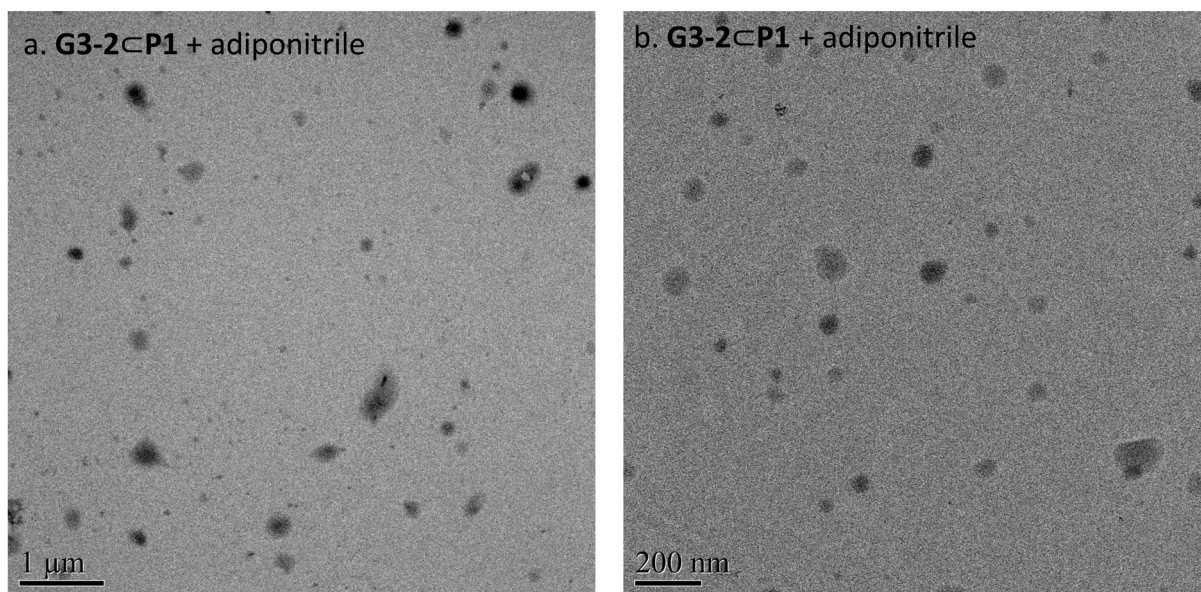


**Figure S34.** TEM images of disaggregated polymeric host-guest suprasphere (G3-2C P1) with the addition of adiponitrile. Shapeless stains with size from hundreds to dozens of nanometers in diameter were observed instead of regular nano-spheres (**Figure 3**)



## Supplementary Equations

### Equations for the binding isotherm

We sequentially choose **RU:GM** 1:1, 2:1 and 3:1 models to fit the binding isotherm determined for the **PASS** systems until the residues between the data and the fit are random around 0. The overall binding constant for **RU:GM** 1:1 complex, **RU:GM** 2:1 complex and **RU:GM** 3:1 complex were represented as  $K_{HG}$ ,  $\beta_{H_2G}$ ,  $\beta_{H_3G}$ . The value of constant for the binding of **RU** to a single arm of **GM** (i.e.  $K$  reported in the paper) was calculated by the following equations under the assumption that the sequential binding of **RU** to the first, the second and the third arm (if available) of **GM** are equal to each other in each **PASS** system.

$$K = K_{HG}$$

$$K = \sqrt{\beta_{H_2G}}$$

$$K = \sqrt[3]{\beta_{H_3G}}$$

### Model 1: RU:Guest 1:1 binding model:

IndVars: [GT]

// [GT]: total guest concentration

DepVars: I, [G], [H], [HG]

Params:  $K_{HG}$ ,  $\Phi_{HG}$ , [H<sub>0</sub>] //

$$[HG] = K_{HG} \times [H] \times [G] \quad 1$$

$$[H] = [H_0] - [HG] \quad 2$$

$$[G] = [GT] - [HG] \quad 3$$

$$I = (\Phi_{HG} - 1) \times [HG] / [H_0] \quad 4$$

// The following section is for the guessing values of parameters.

$$K_{HG} = 9.88 \times 10^5 // \quad 5$$

$$\Phi_{HG} = 8.14 // \quad 6$$

// The following section is for the concentration of RU. .

$$[H_0] = 1.0 \times 10^{-6} // \quad 7$$

// The following section is for the range of the variables.

$$0 < [G] < 1.4 \times 10^{-5} \quad 8$$

$$0 < [H] < 1.3 \times 10^{-5} \quad 9$$

$$0 < [\text{HG}] < 1.3 \times 10^{-5} \quad 10$$

**Model 2: RU:GM 2:1 binding model:**

IndVars: [GT],

// [GT]: total guest concentration

DepVars: I, [H<sub>2</sub>G], [H], [G]

Params:  $\Phi$ , [H<sub>0</sub>],  $\beta_{\text{H}_2\text{G}}$

$$[\text{H}_2\text{G}] = \beta_{\text{H}_2\text{G}} \times [\text{H}]^2 \times [\text{G}] \quad 11$$

$$[\text{H}] = [\text{H}_0] - 2 \times [\text{H}_2\text{G}] \quad 12$$

$$[\text{G}] = [\text{GT}] - [\text{H}_2\text{G}] \quad 13$$

$$I = (2 \times \Phi \times [\text{H}_2\text{G}] + [\text{H}] - [\text{H}_0]) / [\text{H}_0] \quad 14$$

// The following section is for the guessing values of parameters.

$$\beta_{\text{H}_2\text{G}} = 4.88 \times 10^{18} // \quad 15$$

$$\Phi = 8.14 // \quad 16$$

// The following section is for the concentration of RU. .

$$[\text{H}_0] = 1 \times 10^{-6} \quad 17$$

// The following section is for the range of the variables.

$$0 < [\text{G}] < 1 \times 10^{-5} \quad 18$$

$$0 < [\text{H}] < 1 \times 10^{-5} \quad 19$$

$$0 < [\text{H}_2\text{G}] < 1 \times 10^{-5} \quad 20$$

**Model 3: RU:GM 3:1 binding model:**

IndVars: [GT] // [GT]: total guest concentration

DepVars: I, [H<sub>3</sub>G], [H], [G]

Params:  $\Phi$ , [H<sub>0</sub>],  $\beta_{\text{H}_3\text{G}}$

$$[\text{H}_3\text{G}] = \beta_{\text{H}_3\text{G}} \times [\text{H}]^3 \times [\text{G}] \quad 21$$

$$[H] = [H_0] - 3 \times [H_3G] \quad 22$$

$$[G] = [GT] - [H_3G] \quad 23$$

$$I = (3 \times \Phi \times [H_3G] + [H] - [H_0]) / [H_0] \quad 24$$

$$\beta_{H_3G} = 4.88 \times 10^{18} // \quad 25$$

$$\Phi = 8.14 // \quad 26$$

// The following section is for the concentration of RU. .

$$[H_0] = 1 \times 10^{-6} \quad 27$$

// The following section is for the range of the variables.

$$0 < [G] < 1 \times 10^{-5} \quad 28$$

$$0 < [H] < 1 \times 10^{-5} \quad 29$$

$$0 < [H_3G] < 1 \times 10^{-5} \quad 30$$

#### Model 4: Model for the competition experiment:

IndVars: [GcT]

// [GcT]: competitive guest concentration

DepVars: I, [H<sub>3</sub>G], [H], [G], [HGc]

Params:  $\Phi_{HG}$ , [HT], [GT],  $\beta_{H_3G}$ ,  $K_{HGc}$

// [HT]: total concentration of RU; [GT]: total guest concentration.

$$[H_3G] = \beta_{H_3G} \times [H]^3 \times [G] \quad 31$$

$$[HGc] = K_{HGc} \times [H] \times [Gc] \quad 32$$

$$[H] = [HT] - 3 \times [H_3G] - [HGc] \quad 33$$

$$[G] = [GT] - [H_3G] \quad 34$$

$$[Gc] = [GcT] - [HGc] \quad 35$$

$$I = ([H] + 3 \times \Phi_{HG} \times [H_3G] + [HGc]) / ([H]_0 + 3 \times \Phi_{HG} \times [H_3G]_0) \quad 36$$

// The initial values of [H]<sub>0</sub> and [H<sub>3</sub>G]<sub>0</sub> were calculated to be 1.1772 and 2.98418 μM, respectively, under the specific experimental condition using **Scientist 3** with model 3.program.

// The following section is for the guessing values of parameters.

$$\Phi_{HG} = 11 \quad 37$$

$$K_{HGc} = 4.88 \times 10^{-3} \quad 38$$

// The following section is for the variables with known values. .

$$\beta_{H3G} = 1.31 \times 10^{-1} // \text{uM}^{-3} \quad 39$$

$$[HT] = 10 \text{ uM} \quad 40$$

$$[GT] = 16.7 \text{ uM} \quad 41$$

// The following section is for the range of the variables.

$$0 < [G] < 1 \times 10^{-5} \quad 42$$

$$0 < [Gc] < 1 \times 10^{-2} \quad 43$$

$$0 < [H] < 1 \times 10^{-5} \quad 44$$

$$0 < [H3G] < 1 \times 10^{-5} \quad 45$$

*Equations for the relative particle density determined by using m-NTA technology*

As shown in Fig. S32, the raw data determined by using m-NTA technology were given as the dependence of the particle numbers per sample volume ( $[P]$ ) on the diameter of particle ( $d$ ).

$$[P] = f(d) \quad 46$$

The dependence of  $[P]$  on the particle volume ( $V_P$ ) was then determined by equations 46 and 47.

$$V_P = \frac{4}{3} \times \pi \times \left(\frac{d}{2}\right)^3 \quad 47$$

The total particle volume per sample volume ( $V_P^{total}$ ) was determined as the integration of  $[P]$  over  $V_P$  (i.e.  $\sum([P]_i \times V_{P,i})$ ).

The total number of **GMcRU** complex embedded in the **PASS** particles per sample volume ( $[\mathbf{GMcRU}]_{\text{PASS}}$ ) was related to the total number of **GMcRU** complex generated in the samples per sample volume ( $[\mathbf{GMcRU}]_{\text{sample}}$ ) by the following equation :

$$[\mathbf{GMcRU}]_{\text{PASS}} = [\mathbf{GMcRU}]_{\text{sample}} \times a \quad 48$$

where the parameter  $a$  was related to the experimental conditions such as the laser power, frame rate, exposure, video length, the number of videos, as well as other parameters selected. The parameter  $a$  was considered to be the same for the experiments conducted in the same day under the same experimental conditions. The variable of  $[\mathbf{GMcRU}]_{\text{sample}}$  can be calculated according to the model 2 (equations 11-20) or 3 (equations 21-30) aforementioned.

The particle density of the **PASS** ( $\rho$ ) was related to  $[\mathbf{GMcRU}]_{\text{PASS}}$  and  $V_P^{total}$  (equation 49):

$$\rho = \frac{MW_{\mathbf{GMcRU}} \times [\mathbf{GMcRU}]_{\text{PASS}}}{V_P^{total}} \quad 49$$

where  $MW_{\text{GM}\langle\text{RU}\rangle}$  corresponds to the molecular weight of the specific **GM** $\langle$ **RU** $\rangle$  complex.

Equation 50 was derived from equations 48 and 49.

$$\rho = \frac{MW_{\text{GM}\langle\text{RU}\rangle} \times [\text{GM}\langle\text{RU}\rangle]_{\text{sample}} \times a}{V_{\text{p}}^{\text{total}}} \quad 49$$

As a result, the relative particle density for each PASS system ( $RD_i$ ) can be determined by equation 50.

$$RD_i = \frac{\rho_i}{\rho_2} = \frac{MW_i \times [\text{GM}\langle\text{RU}\rangle]_i \times a}{V_{\text{p},i}^{\text{total}}} \times \frac{V_{\text{p},2}^{\text{total}}}{MW_2 \times [\text{GM}\langle\text{RU}\rangle]_2 \times a} \quad 50$$

In this study, the PASS of **G3-2** $\langle$ **RU** $\rangle$  system prepared at 1  $\mu\text{M}$  **RU** and 10  $\mu\text{M}$  **G3-2** was employed as the reference sample, i.e. sample 2 in equation 50. The values of  $RD_i$  were then determined and listed in Table 1 of the paper.

## References

- 1 C. McElfresh, T. Harrington and K. S. Vecchio, *Meas. Sci. Technol.*, 2018, **29**, 065002.
- 2 a) C. Han, Z. Zhang, G. Yu, F. Huang, *Chem. Commun. (Cambridge, U. K.)*, 2012, **48**, 9876; b) M. Pan, M. Xue, *Eur. J. Org. Chem.* 2013, **2013**, 4787; c) W. Wu, S. Ye, R. Tang, L. Huang, Q. Li, G. Yu, Y. Liu, J. Qin, Z. Li, *Polymer*, 2012, **53**, 3163; d) S.-L. Li, T. Xiao, B. Hu, Y. Zhang, F. Zhao, Y. Ji, Y. Yu, C. Lin, L. Wang, *Chem. Commun. (Cambridge, U. K.)*, 2011, **47**, 10755; e) Z.-Y. Li, Y. Zhang, C.-W. Zhang, L.-J. Chen, C. Wang, H. Tan, Y. Yu, X. Li, H.-B. Yang, *J. Am. Chem. Soc.*, 2014, **136**, 8577.
- 3 C. Li, K. Han, J. Li, Y. Zhang, W. Chen, Y. Yu, X. Jia, *Chem. - Eur. J.*, 2013, **19**, 11892.